Available online at www.sciencedirect.com

ScienceDirect

Journal of Differential Equations 323 (2022) 280–311

Journal of Differential Equations

www.elsevier.com/locate/jde

Bifurcations in the diffusive Bazykin model

Min Lu [a], Chuang Xiang [a], Jicai Huang [a,*], Hao Wang [b,*]

[a] School of Mathematics and Statistics, Central China Normal University, Wuhan, Hubei 430079, PR China

[b] Department of Mathematical and Statistical Sciences, University of Alberta, Edmonton, Alberta T6G 2G1, Canada

Received 28 November 2021; revised 25 March 2022; accepted 26 March 2022

Abstract

Dangerous tipping points and catastrophic transitions in ecosystems have recently been popular for detecting early warning signals in ecology. B-tipping is induced by bifurcation such as spatial pattern formation resulting from Turing instability. As one of the most important models in predator-prey interactions, we extend the Bazykin model to incorporate diffusive movement under homogeneous Neumann boundary conditions. For the local model, we provide some preliminary analysis on stability and Hopf bifurcation. For the reaction-diffusion model, we first improve some sufficient conditions for the local and global stability of a semi-trivial constant steady state or a unique positive constant steady state in Du and Lou (2001) [11]. Next we obtain the sufficient and necessary conditions for Turing instability, show the existence of Turing bifurcation, Hopf bifurcation, Turing-Turing bifurcation, Turing-Hopf bifurcation and Turing-Turing-Hopf bifurcation, and the nonexistence of triple-Turing bifurcation. Our results reveal that the model can exhibit complex spatial, temporal and spatiotemporal patterns, including complex regime shifts and critical transitions at bifurcation points, transient states (spatially inhomogeneous periodic solutions), tristability (a pair of non-constant steady states and a spatially homogeneous periodic solution), heteroclinic orbits (connecting a spatially inhomogeneous periodic solution to a non-constant steady state or a spatially homogeneous periodic solution, connecting a spatially homogeneous periodic solution to non-constant steady states and vice versa). Finally, numerical simulations illustrate complex dynamics and verify our theoretical results.

Keywords: Diffusive Bazykin model; Turing instability; Bifurcations; Tipping points; Regime shifts; Critical transitions

* Corresponding authors.
E-mail addresses: hao8@ualberta.ca (H. Wang), hjc@mail.ccnu.edu.cn (J. Huang).

https://doi.org/10.1016/j.jde.2022.03.039
0022-0396/

1. Introduction

Ecosystems on the earth are undergoing severe global climate and land-use change, therefore there is an increasing need to better understand the impact of these changes. Tipping points and critical transitions help understand the catastrophic effects on ecosystems [40]. Tipping points are critical thresholds at which the system shifts abruptly from one stable state (often desired) to another (often unfavorable), and fundamental shifts that occur in the system when they pass bifurcations (collectively referred to as critical transitions) [41,43]. There are some classical ecosystem examples to exhibit critical transitions with tipping points between alternative stable states, such as clear lakes becoming turbid because of nutrient overloading [42], and barren deserts replacing vegetated areas in dry savannas or drylands because of drought or overgrazing [39]. Hence the detection of early warning signals for such transitions has become an urgent, cutting-edge direction in ecology. B-tipping is caused by bifurcation for which some key parameters shift across threshold values and reduce the basin of attraction of an original stable state to zero [40]. Such key parameters and threshold values are called bifurcation parameters and bifurcation values in bifurcation theory, respectively [29]. For example, spatial pattern formation resulting from Turing instability has been used as an early warning signal for dangerous tipping points and imminent critical transitions in complex ecosystems [40].

Lotka in 1925 [31] and Volterra in 1926 [48] independently proposed the best-known Lotka-Volterra (L-V) predator-prey model, which has become the fundamental base for many subsequent predator-prey models. To reflect the realistic mechanisms in different types of predation, the original L-V model has been refined and extended to incorporate many new, important ecological relationships and environmental factors. Among them, by taking prey's intraspecific competition, predator competition due to crowding effect, and different functional responses into account, the classical L-V model became the generalized predator-prey system [16]:

$$
\begin{aligned}
\frac{dx}{dt} &= ax(1-\frac{x}{K}) - yp(x,y),\\
\frac{dy}{dt} &= y(-c+dp(x,y)) - hy^2,
\end{aligned}
\tag{1.1}
$$

where $x(t)$ and $y(t)$ represent the population densities of the prey and predators at time t, respectively; $ax(1-\frac{x}{K})$ denotes the specific growth of the prey in the absence of predators, a is the intrinsic growth rate, K is the carrying capacity; $h>0$ is the coefficient of predator competition due to self-limitation; $p(x,y)$ is the functional response describing the change in the density of prey attacked per unit time by one predator.

System (1.1) with different functional responses has been studied extensively, see for example, Bazykin [3] for Lotka-Volterra type: $p(x,y)=bx$; Bazykin et al. [3,4], Hainzl [19], Kuznetsov [29], Lu and Huang [32] for Holling type II: $p(x,y)=\frac{bx}{1+Ax}$; Freedman [15], Bazykin [4] for Holling type III: $p(x,y)=\frac{bx^2}{1+Ax^2}$; Broer et al. [5] for generalized Holling type IV: $p(x,y)=\frac{bx}{1+Bx+Ax^2}$ $(B>-2\sqrt{A})$; Haque [21], Jiang et al. [27] for ratio-dependent type: $p(x,y)=\frac{mx}{ax+by}$; Haque [22], Zhang and Huang [58] for Beddington-DeAngelis type: $p(x,y)=\frac{mx}{ax+by+c}$. It was shown that system (1.1) can undergo complex dynamical behaviors and bifurcation phenomena even for Holling type II functional response [32], such as a big limit cycle enclosing three hyperbolic positive equilibria and a small homoclinic loop, or a huge homoclinic loop connecting a hyperbolic saddle and enclosing two hyperbolic positive equilibria, or two big limit cycles enclosing three hyperbolic positive equilibria, or a big limit cycle enclosing three hyperbolic positive equilibria and a small limit cycle, three kinds of homoclinic loops (homoclinic to hyperbolic saddle, saddle-node, or neutral saddle), Hopf bifurcation with codimension up to 2, focus type degenerate Bogdanov-Takens bifurcation of codimension 3, etc.

In reality, species move in their habitats, and the simplest way is random Brownian motion that can modeled by symmetric diffusion. Diffusive predator-prey systems with different functional responses were extensively studied, for instance, Du and Hsu [10], Peng and Wang [38] for Lotka-Volterra type and spatially homogeneity; Du and Lou [11] for Holling II type and spatially homogeneity; Du and Shi [12] for Holling II type and spatially heterogeneity; Vales [1], Haque [23], Min et al. [33] for Beddington-DeAngelis type; Zhou [59], Cao and Jiang [7] for Crowley-Martin type; Wang [51], Zeng et al. [57] for ratio-dependent type, etc. Specifically, Du and Lou [11] studied positive steady-state solutions of the system with Holling type II functional response:

$$\begin{cases} u_t - d_1 \Delta u = u(a - u - bv/(1+mu)), & x \in \Omega,\ t > 0, \\ v_t - d_2 \Delta v = v(d - v + cu/(1+mu)), & x \in \Omega,\ t > 0, \\ \dfrac{\partial u}{\partial \nu} = \dfrac{\partial v}{\partial \nu} = 0, & x \in \partial\Omega,\ t > 0, \end{cases} \tag{1.2}$$

where the given coefficients are all positive except d. If $d > 0$, the predator (generalist) can survive in the absence of prey; otherwise, the predator (specialist) will go extinct in the absence of prey. For $d_1 = d_2 = 0$ (no diffusion) and $d < 0$, model (1.2) is called the Bazykin model, i.e., model (1.1) with Holling type II functional response. For $m = 0$, Leung [30] proved that all positive solutions of (1.2), regardless of the initial data, converge to a constant steady state solution as time goes to infinity, which means that the case $m = 0$ does not give rise to any interesting phenomenon. The results also hold for a small positive m [6,34]. Du and Lou [11] studied the mutual effect of d and large m on the existence and nonexistence of non-constant positive steady states. Supposing $d_1 = 1$ and $d < 0$, Banerjee et al. [2] gave a necessary and insufficient condition for Turing bifurcation, and used approximated analytical solution as the initial condition to obtain spiral and target patterns via numerical simulations. When $d_1 = 1$ and $d < 0$, Pal et al. [36] considered the effect of a nonlocal interaction term in prey growth, first gave a necessary and insufficient condition for Turing bifurcation, and then got the amplitude equations to study spatial patterns by combining weakly nonlinear analysis and numerical simulations. Although plentiful results about stability of a constant steady state, the existence and nonexistence of non-constant positive steady states, Turing bifurcation and Turing pattern, have been revealed for system (1.2), the nonlinear dynamics and complex bifurcation phenomena of system (1.2) are not well understood. We list the unknown questions in the following:

- Can the results in [11] about the global stability be improved?
- Can we obtain the sufficient and necessary condition for Turing bifurcation?
- Hopf bifurcation: the direction and stability of bifurcating periodic solutions in system (1.2) and the corresponding local system. Are the stability and direction of 0-mode Hopf bifurcation in system (1.2) the same as those of the corresponding local system?
- Bifurcations for high codimension: can we obtain Turing-Turing bifurcation, Turing-Hopf bifurcation, Turing-Turing-Hopf bifurcation, triple-Turing bifurcation?

- Are there complex regime shifts and critical transitions around tipping points (B-tipping, i.e., Turing bifurcation point and Turing-Hopf bifurcation point)?

To rigorously answer these questions, we consider the diffusive Bazykin model (i.e., $d < 0$ in (1.2)):

$$\begin{cases} U_t - D_1 \Delta U = aU(1 - \dfrac{U}{K}) - \dfrac{bUV}{1 + AU}, & x \in \Omega,\ t > 0, \\ V_t - D_2 \Delta V = -cV + \dfrac{dUV}{1 + AU} - hV^2, & x \in \Omega,\ t > 0, \\ \dfrac{\partial U}{\partial \nu} = \dfrac{\partial V}{\partial \nu} = 0, & x \in \partial\Omega,\ t > 0, \\ U(x,0) = U_0(x) \geq 0,\ V(x,0) = V_0(x) \geq 0, & x \in \Omega, \end{cases} \tag{1.3}$$

where Ω is a bounded domain in $\mathbb{R}^N$, $N \geq 1$, with smooth boundary $\partial\Omega$, $\nu(x)$ denotes the unit outward normal vector at $x \in \partial\Omega$ and $\Delta = \sum_{i=1}^{N} \frac{\partial^2}{\partial x_i^2}$ is the usual Laplace operator. The Neumann boundary condition indicates that no individuals can move across $\partial\Omega$, i.e., the habitat is closed. Here, $U(x,t)$ and $V(x,t)$ stand for the densities of prey and the predator at time $t > 0$ and a spatial position $x \in \Omega$, respectively. $D_1,\ D_2 > 0$ are the diffusion coefficients of the species. The parameters $a,\ b,\ c,\ d,\ A,\ K,\ h$ are all positive: a is the reproduction rate of the prey population in the absence of the predator, K is the carrying capacity, c is the natural mortality rate of the predator, h is the coefficient of predator competition for crowding effect, $\frac{b}{A}$ is the maximum consumption of the predator, A reflects a growing saturation effect of the predator when the prey density is increasing, $\frac{1}{A}$ is the prey density at which the predator's consumption is half of the maximum value, and $\frac{d}{b}$ is the conversion efficiency from prey to the predator.

From [44–46,54], we observe that codimension-2 Turing-Hopf bifurcation can induce numerous interesting spatiotemporal patterns. Usually, [13,14,18,20,52] use the normal form method to investigate dynamics of differential systems. Due to the complexities of calculating normal forms, Jiang [25], Song [45] and Yang [54] derived several concise formulas of calculating normal forms for partial functional differential equations and partial differential equations at Turing-Hopf singularity, respectively. Diffusive systems can exhibit rich spatial dynamics by Turing bifurcation and numerous interesting spatial, temporal and spatiotemporal patterns by Turing-Hopf bifurcation. Following Alan Turing's pioneering paper [47], many scholars discovered spatial and spatiotemporal patterns in chemical reaction-diffusion models and diffusive predator-prey models, see [9,26,28,35,37,49,50,54,55]. According to [17], there are twelve unfoldings for normal forms of diffusive systems at Turing-Hopf singularity in total, depending on cubic coefficients of normal forms.

Before expanding details, we rescale system (1.3) by

$$U = Ku, \quad V = \frac{a}{h}v, \quad t = \frac{1}{a}\tau, \quad u_0(x) = \frac{U_0(x)}{K}, \quad v_0(x) = \frac{hV_0(x)}{a}, \tag{1.4}$$

then system (1.3) becomes (still denote τ by t)

$$
\begin{cases}
u_t - d_1 \Delta u = u(1-u) - \dfrac{\beta u v}{\alpha + u}, & x \in \Omega,\ t > 0, \\
v_t - d_2 \Delta v = -\delta v + \dfrac{\gamma u v}{\alpha + u} - v^2, & x \in \Omega,\ t > 0, \\
\dfrac{\partial u}{\partial \nu} = \dfrac{\partial v}{\partial \nu} = 0, & x \in \partial\Omega,\ t > 0, \\
u(x,0) = u_0(x) \geq 0,\ v(x,0) = v_0(x) \geq 0, & x \in \Omega,
\end{cases}
\tag{1.5}
$$

where

$$
d_1 = \frac{D_1}{a}, \quad d_2 = \frac{D_2}{a}, \quad \alpha = \frac{1}{AK}, \quad \beta = \frac{b}{AhK}, \quad \gamma = \frac{d}{Aa}, \quad \delta = \frac{c}{a}, \tag{1.6}
$$

and d_1, d_2, α, β, γ, δ are all positive parameters. Firstly, we will give some new results for the global stability of a prey-only constant steady state or a unique positive constant steady state, which improve the corresponding ones in Du and Lou (2001) [11]. Secondly, we will obtain the sufficient and necessary conditions for Turing instability and Turing bifurcation. Moreover, we will give a more concise definition of the critical wavelengths for the Turing instability. Thirdly, we will study Hopf bifurcation in system (1.5) and the corresponding local system, and show that the stability and direction of 0-mode Hopf bifurcation in system (1.5) are the same as those of the corresponding local system. Fourthly, we will rigorously study bifurcations for high codimension in system (1.5), including the existence of Turing-Turing bifurcation, Turing-Hopf bifurcation, Turing-Turing-Hopf bifurcation, and the nonexistence of triple-Turing bifurcation. Moreover, we will obtain the explicit formula of normal form up to the third order for Turing-Hopf bifurcation, and show that the unfolding for normal form is similar to Case Ib in section 7.5 of [17]. Finally, we will show that complex regime shifts and critical transitions occur around a tipping point (B-tipping), i.e., Turing-Hopf bifurcation point, which is located on the Turing bifurcation curve, for example, a stable constant steady state to a stable spatially homogeneous periodic solution, or a stable constant steady state to one of two stable non-constant steady states depending on the initial values, or a stable constant steady state to one of two stable non-constant steady states or to a stable spatially homogeneous periodic solution depending on the initial values. System (1.5) can undergo from monostability to bistability, even tristability. Moreover, system (1.5) can exhibit complex transient dynamics, such as transient spatially inhomogeneous periodic solutions, etc.

The rest of the paper is organized as follows. In section 2, we present preliminary analysis on the stability and Hopf bifurcation of the local system. In section 3, we provide some sufficient conditions to guarantee the global stability of the boundary constant steady state or the unique positive constant steady state for the reaction-diffusion model (1.5). In section 4, we show that the system exhibits Turing bifurcation, which will produce spatial inhomogeneous patterns, and give the sufficient and necessary conditions for the occurrence of Turing instability. Then we obtain the existence and direction of Hopf bifurcation and the stability of the bifurcating periodic solution, which is a spatially homogeneous periodic solution of the reaction-diffusion model (1.5) and exhibits temporal periodic patterns. In section 5, we investigate Turing-Turing bifurcation and Turing-Hopf bifurcation of the reaction-diffusion model (1.5) which will produce spatiotemporal patterns, and derive the explicit formula of truncated normal form up to third order for Turing-Hopf bifurcation. A detailed analysis reveals that the model exhibits spatial, temporal, and spatiotemporal patterns, including transient spatially inhomogeneous periodic solutions, as well as tristable phenomena in the coexistence of a pair of positive non-constant steady states and a spatially homogeneous periodic solution. Meanwhile, numerical simulations illustrate and verify our theoretical results. A brief discussion is given in the last section.

2. Stability and Hopf bifurcation of the local system

In this section, we study system (1.5) without diffusion, i.e., the local system

$$\begin{cases} u_t = u(1-u) - \dfrac{\beta u v}{\alpha + u} \triangleq f(u,v), \\[2ex] v_t = -\delta v + \dfrac{\gamma u v}{\alpha + u} - v^2 \triangleq g(u,v). \end{cases} \tag{2.1}$$

Notice that system (2.1) always has two boundary equilibria $A_1(0,0)$ and $A_2(1,0)$ for all parameters. The Jacobian matrix of system (2.1) at any equilibrium $E(u,v)$ is

$$J = \begin{pmatrix} f_u & f_v \\ g_u & g_v \end{pmatrix}. \tag{2.2}$$

Then Jacobian matrix of system (2.1) at $A_1(0,0)$ and $A_2(1,0)$ takes respectively the form

$$J(A_1) = \begin{pmatrix} 1 & 0 \\ 0 & -\delta \end{pmatrix}, \quad J(A_2) = \begin{pmatrix} -1 & -\frac{\beta}{\alpha+1} \\ 0 & -\delta + \frac{\gamma}{\alpha+1} \end{pmatrix}. \tag{2.3}$$

We list the basic results of the stability for system (2.1) in [32] as follows.

Lemma 2.1. *System (2.1) always has two boundary equilibria $A_1(0,0)$ and $A_2(1,0)$. Moreover, $A_1(0,0)$ is always a hyperbolic saddle, and*

- **(i)** *if $\delta < \frac{\gamma}{\alpha+1}$, then $A_2(1,0)$ is a hyperbolic saddle;*
- **(ii)** *if $\delta > \frac{\gamma}{\alpha+1}$, then $A_2(1,0)$ is a hyperbolic stable node;*
- **(iii)** *if $\delta = \frac{\gamma}{\alpha+1}$, then $A_2(1,0)$ is a saddle-node which includes a stable parabolic sector lies in the upper half plane.*

Lemma 2.2. *When $\delta \geq \frac{\gamma}{\alpha+1}$, then the boundary equilibrium $A_2(1,0)$ of system (2.1) is globally asymptotically stable in the interior of $\mathbb{R}_2^+$.*

Next, we consider the case $\delta < \frac{\gamma}{\alpha+1}$. Let

$$\begin{aligned} F(u) &= u^3 + (2\alpha - 1)u^2 + (\alpha^2 - 2\alpha + \beta\gamma - \beta\delta)u - \alpha(\alpha + \beta\delta), \\ G(u) &= \frac{\mathrm{d}F(u)}{\mathrm{d}u} = 3u^2 + 2(2\alpha - 1)u + (\alpha^2 - 2\alpha + \beta\gamma - \beta\delta). \end{aligned} \tag{2.4}$$

From [32], system (2.1) has a unique positive equilibrium $E^*(u^*, v^*)$ if $\alpha \geq \frac{1}{2}$ and $\delta < \frac{\gamma u^*}{\alpha+u^*}$, where $u^* \in (0, 1)$ is the unique positive root of $F(u) = 0$ and $v^* = -\delta + \frac{\gamma u^*}{\alpha+u^*}$. Noting that $\frac{\gamma u^*}{\alpha+u^*} < \frac{\gamma}{\alpha+1}$ for $0 < u^* < 1$. Therefore, a sufficient condition for system (2.1) to has a unique positive equilibrium $E^*(u^*, v^*)$ is $(\alpha, \beta, \gamma, \delta) \in U_1$, where

$$U_1 = \{(\alpha, \beta, \gamma, \delta) \mid \beta > 0,\ \gamma > 0,\ \alpha \geq \frac{1}{2},\ 0 < \delta < \frac{\gamma u^*}{\alpha + u^*}\}. \tag{2.5}$$

A straight calculation yields the Jacobian matrix of system (2.1) at $E^*(u^*, v^*)$ is

$$J(E^*) = \begin{pmatrix} \overline{A} & \overline{B} \\ \overline{C} & \overline{D} \end{pmatrix}$$

where

$$\overline{A} = \frac{u^*(1-2u^*-\alpha)}{\alpha+u^*}, \quad \overline{B} = -\frac{\beta u^*}{\alpha+u^*} < 0, \quad \overline{C} = \frac{\gamma\alpha(1-u^*)}{\beta(\alpha+u^*)} > 0, \quad \overline{D} = \delta - \frac{\gamma u^*}{\alpha+u^*} < 0. \tag{2.6}$$

Let

$$\beta = \beta^* \triangleq \frac{(1-u^*)(u^*+\alpha)^2}{\gamma u^* - (u^*+\alpha)\delta},$$

which obtains from $F(u^*) = 0$. It is easily to see that the determinant of $J(E^*)$ and $G(u^*)$ satisfy

$$\mathrm{Det}_0 \triangleq \mathrm{Det}(J(E^*)) = \frac{u^*(\gamma u^* - (\alpha+u^*)\delta)}{\alpha+u^*} G(u^*)|_{\beta=\beta^*}, \tag{2.7}$$

which implies $\mathrm{Det}_0 > 0$. Let

$$\mathrm{Tr}_0 \triangleq \mathrm{Tr}(J(E^*)) = \frac{u^*(-2u^*+1-\alpha-\gamma)+\delta(u^*+\alpha)}{\alpha+u^*}, \quad \delta_0 = \frac{u^*(2u^*-1+\alpha+\gamma)}{\alpha+u^*}. \tag{2.8}$$

Then we have the following results.

Lemma 2.3. *If $(\alpha, \beta, \gamma, \delta) \in U_1$, then the unique positive equilibrium $E^*(u^*, v^*)$ of system (2.1) is locally asymptotically stable if $\mathrm{Tr}_0 < 0$, and unstable if $\mathrm{Tr}_0 > 0$. More precisely,*

- **(i)** *if $u^* \geq \frac{1-\alpha}{2}$, then $E^*(u^*, v^*)$ is locally asymptotically stable;*
- **(ii)** *if $\frac{1-\alpha-\gamma}{2} < u^* < \frac{1-\alpha}{2}$ and*
  - **(a)** *$\delta < \delta_0$, then $E^*(u^*, v^*)$ is locally asymptotically stable;*
  - **(b)** *$\delta = \delta_0$, then $E^*(u^*, v^*)$ is a center-type equilibrium;*
  - **(c)** *$\delta > \delta_0$, then $E^*(u^*, v^*)$ is unstable;*
- **(iii)** *if $u^* \leq \frac{1-\alpha-\gamma}{2}$, then $E^*(u^*, v^*)$ is unstable.*

We next consider case (ii)(b) in Lemma 2.3, the transversality condition for Hopf bifurcation around E^* is

$$\frac{1}{2}\frac{\mathrm{d}}{\mathrm{d}\delta}(\mathrm{Tr}_0)\mid_{\delta=\delta_0}=\frac{1}{2}>0.$$

Using the formula in [17] to calculate the first Lyapunov coefficient with the aid of MATLAB software, we obtain

$$\sigma_1=\frac{(1-u^*)^2u^*\sigma_{11}}{4(\alpha+u^*)^3(-1+2u^*+\alpha)^2(\mathrm{Det}_0)^{3/2}}.$$

Obviously, the sign of σ_1 is the same as

$$\begin{aligned}\sigma_{11}=&-2\alpha^3\gamma-\alpha\left(-\alpha^2+\alpha(\gamma+2)+\gamma-1\right)u^*+(1-\alpha)\alpha(3\alpha+3\gamma-5)u^{*2}\\&-4\alpha(3\alpha+\gamma-3)u^{*3}-2(7\alpha-1)u^{*4}-4u^{*5}.\end{aligned}\tag{2.9}$$

We have the following results.

Lemma 2.4. *Let $\delta=\delta_0$, $\frac{1-\alpha-\gamma}{2}<u^*<\frac{1-\alpha}{2}$ and $(\alpha,\beta,\gamma,\delta)\in U_1$, then we have*

- **(I)** *If $\sigma_{11}<0$, then $E^*(u^*,v^*)$ is a stable weak focus with multiplicity 1, and system (2.1) can exhibit supercritical Hopf bifurcation around E^*;*
- **(II)** *If $\sigma_{11}>0$, then $E^*(u^*,v^*)$ is an unstable weak focus with multiplicity 1, and system (2.1) can exhibit subcritical Hopf bifurcation around E^*.*

Now we give some numerical simulations for above analysis. Firstly, we fixed $\alpha=\frac{3}{4}$, $\gamma=\frac{1}{4}$, $u^*=\frac{1}{16}$, and get $\delta_0=\frac{1}{104}$. When $\delta=\delta_0=\frac{1}{104}$, we have $\sigma_1=-\frac{13551075}{5728\sqrt{179}}$, which implies that $E^*(u^*,v^*)$ of system (2.1) is a stable weak focus with multiplicity 1. In Fig. 2.1(a), E^* is stable when $\delta=\frac{1}{104}-\frac{1}{1000}<\delta_0$. In Fig. 2.1(b), E^* is unstable and encircled by a stable limit cycle bifurcating from supercritical Hopf bifurcation when $\delta=\frac{1}{104}+\frac{1}{1000}>\delta_0$.

Moreover, we cite the following result for global asymptotical stability of $E^*(u^*,v^*)$ from [32].

Lemma 2.5. *If $\delta<\frac{\gamma}{\alpha+1}$ and $E^*(u^*,v^*)$ is an interior equilibrium of system (2.1) with $u^*\geq 1-\alpha$, then E^* is the unique positive equilibrium of system (2.1) and it is globally asymptotically stable in the interior of $\mathbb{R}_2^+$.*

3. Local and global stability of reaction-diffusion system

In this section, we consider one-dimensional spatial domain $\Omega=(0,l\pi)$, $l\in\mathbb{R}^+$ for system (1.5):

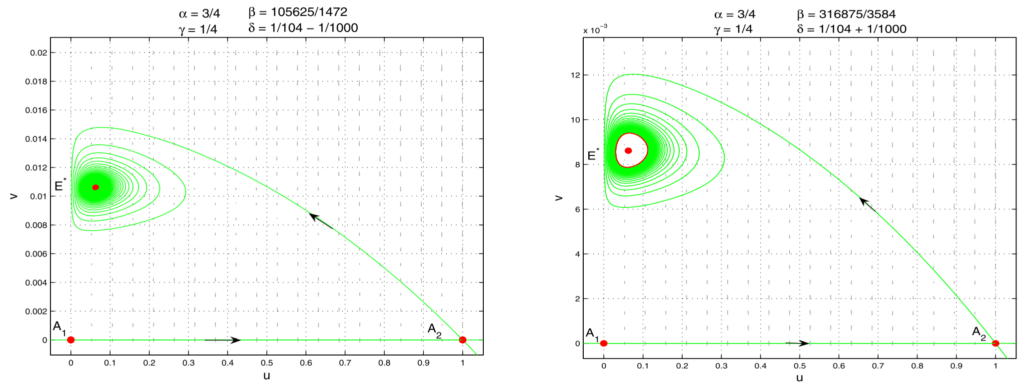

(a) (b)

Fig. 2.1. (a) $E^*(u^*, v^*)$ of system (2.1) is stable if $\delta < \delta_0$; (b) E^* is unstable and encircled by a stable limit cycle if $\delta > \delta_0$.

$$
\begin{cases}
u_t - d_1 u_{xx} = u(1-u) - \dfrac{\beta u v}{\alpha + u}, & x \in (0, l\pi),\ t > 0, \\
v_t - d_2 v_{xx} = -\delta v + \dfrac{\gamma u v}{\alpha + u} - v^2, & x \in (0, l\pi),\ t > 0, \\
u_x(0,t) = v_x(0,t) = 0,\ u_x(l\pi, t) = v_x(l\pi, t) = 0, & t > 0, \\
u(x,0) = u_0(x) \geq 0,\ v(x,0) = v_0(x) \geq 0, & x \in (0, l\pi).
\end{cases}
\tag{3.1}
$$

System (3.1) always has two boundary constant steady states: $A_1(0,0)$, $A_2(1,0)$, and a unique positive constant steady state $E^*(u^*, v^*)$ if $(\alpha, \beta, \gamma, \delta) \in U_1$, where U_1 is given in (2.5).

Define the real-valued Sobolev space

$$
X := \left\{ (u, v) \in H^2(0, l\pi) \times H^2(0, l\pi) \,\middle|\, (u_x, v_x)|_{x=0,\ l\pi} = 0 \right\},
$$

and the complexification of X to be $X_{\mathbb{C}} := X \oplus iX = \{x_1 + i x_2 \,|\, x_1, x_2 \in X\}$.

The linearized system of system (3.1) at (u, v) is

$$
\begin{pmatrix} u_t \\ v_t \end{pmatrix} = L \begin{pmatrix} u \\ v \end{pmatrix} = \hat{D} \begin{pmatrix} u_{xx} \\ v_{xx} \end{pmatrix} + J \begin{pmatrix} u \\ v \end{pmatrix} \tag{3.2}
$$

where $\hat{D} = \mathrm{diag}(d_1, d_2)$, J is the Jacobian matrix defined in Section 2, and L is a linear operator with domain $D_L = X_{\mathbb{C}}$.

Let

$$
\begin{pmatrix} \phi \\ \psi \end{pmatrix} = \sum_{k=0}^{\infty} \cos\frac{k}{l} x \begin{pmatrix} a_k \\ b_k \end{pmatrix} \tag{3.3}
$$

be an eigenfunction for L with eigenvalue λ, that is, $L(\phi, \psi)^T = \lambda(\phi, \psi)^T$. Then a straightforward calculation yields

$$L_k \begin{pmatrix} a_k \\ b_k \end{pmatrix} = \lambda \begin{pmatrix} a_k \\ b_k \end{pmatrix}, \ k = 0, 1, 2, \cdots, \tag{3.4}$$

where

$$L_k = J - \frac{k^2}{l^2} \hat{D}. \tag{3.5}$$

It is clear that the eigenvalues of the operator L are given by the eigenvalues of the matrix L_k. The characteristic equation of L_k is

$$\lambda^2 - (\mathrm{Tr}_k)\lambda + \mathrm{Det}_k = 0, \quad k = 0, 1, 2, \cdots, \tag{3.6}$$

where

$$\begin{cases} \mathrm{Tr}_k = f_u + g_v - \dfrac{(d_1 + d_2)k^2}{l^2}, \\ \mathrm{Det}_k = d_1 d_2 \dfrac{k^4}{l^4} - \dfrac{k^2}{l^2}(d_2 f_u + d_1 g_v) + f_u g_v - f_v g_u, \end{cases} \tag{3.7}$$

and the eigenvalues λ are given by

$$\lambda = \frac{\mathrm{Tr}_k \pm \sqrt{(\mathrm{Tr}_k)^2 - 4\mathrm{Det}_k}}{2}, \quad k = 0, 1, 2, \cdots. \tag{3.8}$$

We have the following results for the local stability of the boundary constant steady states $A_1(0, 0)$ and $A_2(1, 0)$.

Lemma 3.1. *The constant steady state $A_1(0, 0)$ of system (3.1) is unstable, the constant steady state $A_2(1, 0)$ is asymptotically stable if $\delta > \frac{\gamma}{\alpha+1}$, and is unstable if $\delta < \frac{\gamma}{\alpha+1}$.*

Proof. According to (3.5), we have $L_k(A_1) = J(A_1) - \frac{k^2}{l^2}\hat{D}$ and $L_k(A_2) = J(A_2) - \frac{k^2}{l^2}\hat{D}$, then the trace and determinant of $L_k(A_1)$ and $L_k(A_2)$ are

$$\begin{cases} \mathrm{Tr}_k(A_1) = 1 - \delta - \dfrac{(d_1 + d_2)k^2}{l^2}, \\ \mathrm{Det}_k(A_1) = d_1 d_2 \dfrac{k^4}{l^4} - \dfrac{k^2}{l^2}(d_2 - d_1\delta) - \delta, \end{cases}$$

$$\begin{cases} \mathrm{Tr}_k(A_2) = -1 - (\delta - \dfrac{\gamma}{\alpha + 1}) - \dfrac{(d_1 + d_2)k^2}{l^2}, \\ \mathrm{Det}_k(A_2) = d_1 d_2 \dfrac{k^4}{l^4} + \dfrac{k^2}{l^2}(d_2 + d_1(\delta - \dfrac{\gamma}{\alpha + 1})) + \delta - \dfrac{\gamma}{\alpha + 1}. \end{cases}$$

It is easy to see that $\mathrm{Det}_0(A_1) = -\delta < 0$, $\mathrm{Det}_0(A_2) < 0$ if $\delta < \frac{\gamma}{\alpha+1}$, $\mathrm{Det}_k(A_2) > 0$ and $\mathrm{Tr}_k(A_2) < 0$ if $\delta > \frac{\gamma}{\alpha+1}$. Thus we reach the conclusions. $\square$

Furthermore, we have the following global stability results about $A_2(1,0)$.

Theorem 3.2. *Suppose that $\delta \geq \frac{\gamma}{\alpha+1}$, then $A_2(1,0)$ of system (3.1) is globally stable.*

Proof. We define

$$E(u(x,t),v(x,t)) = \frac{\gamma}{\beta}\int_\Omega \int_1^u \frac{\Phi(\xi)-\Phi(1)}{\Phi(\xi)} d\xi dx + \int_\Omega v dx,$$

where $\Phi(u) = \frac{\beta u}{\alpha+u}$. Then

$$\begin{aligned} E_t(u,v) &= \frac{\gamma}{\beta}\int_\Omega \frac{\Phi(u)-\Phi(1)}{\Phi(u)} u_t dx + \int_\Omega v_t dx \\ &= \int_\Omega \Big[-\frac{\gamma\alpha(1-u)^2}{\beta(\alpha+1)} - v^2 - v(\delta - \frac{\gamma}{\alpha+1}) \Big] dx + I_1(t), \end{aligned}$$

where

$$\begin{aligned} I_1(t) &= \frac{d_1\gamma}{\beta}\int_\Omega \frac{\Phi(u)-\Phi(1)}{\Phi(u)} \Delta u dx + d_2 \int_\Omega \Delta v dx \\ &= -\frac{d_1\gamma}{\beta}\int_\Omega \frac{\Phi'(u)\Phi(1)}{\Phi^2(u)} |\nabla u|^2 dx. \end{aligned}$$

Notice that $\Phi'(u) > 0$ for $u \geq 0$. Thus, when $\delta \geq \frac{\gamma}{\alpha+1}$, $E_t \leq 0$ along an orbit $(u(x,t), v(x,t))$ of system (3.1) with positive initial value (u_0, v_0), and $E_t = 0$ if and only if $(u(x,t), v(x,t)) = (1,0)$. Therefore, we complete the proof. □

Remark 3.3. Our results in Theorem 3.2 improve the one in Du and Lou [11], where they showed that $A_2(1,0)$ is globally attractive if $\delta \geq \frac{\gamma}{\alpha+1}$ and $\alpha \geq 1$.

Hence, we assume that $(\alpha,\beta,\gamma,\delta) \in U_1$ in the following analysis, then there exists a unique positive constant steady state $E^*(u^*, v^*)$ for system (3.1). According to (3.5), we have $L_k(E^*) = J(E^*) - \frac{k^2}{l^2}\hat{D}$, then the characteristic equation of $L_k(E^*)$ is

$$P_k(\lambda) = \lambda^2 - \lambda \mathrm{Tr}_k(E^*) + \mathrm{Det}_k(E^*) = 0, \quad k = 0,1,2,\cdots, \tag{3.9}$$

where

$$\begin{cases} \mathrm{Tr}_k(E^*) = \overline{A} + \overline{D} - \dfrac{(d_1+d_2)k^2}{l^2}, \\ \mathrm{Det}_k(E^*) = d_1 d_2 \dfrac{k^4}{l^4} - \dfrac{k^2}{l^2}(\overline{A} d_2 + d_1 \overline{D}) + \overline{A}\,\overline{D} - \overline{B}\,\overline{C}, \end{cases}$$

and $\overline{A}, \overline{B}, \overline{C}, \overline{D}$ are given in (2.6). For the sake of convenience, define

$$\varphi(\frac{k^2}{l^2}) \triangleq \mathrm{Det}_k(E^*) = d_1 d_2 \frac{k^4}{l^4} - \frac{k^2}{l^2}(\overline{A}d_2 + d_1\overline{D}) + \overline{A}\,\overline{D} - \overline{B}\,\overline{C}, \tag{3.10}$$

which is a quadratic polynomial with respect to $\frac{k^2}{l^2}$.

It is clear that if $u^* \geq \frac{1-\alpha}{2}$, i.e., $\overline{A} \leq 0$, then $\overline{A} + \overline{D} < 0$ and $\overline{A}d_2 + d_1\overline{D} < 0$, which implies $\mathrm{Tr}_k(E^*) < 0$ and $\varphi(\frac{k^2}{l^2}) > 0$ for any $k > 0$ since $\overline{A}\,\overline{D} - \overline{B}\,\overline{C} > 0$. Then we have the following result.

Theorem 3.4. *If $u^* \geq \frac{1-\alpha}{2}$ and $(\alpha, \beta, \gamma, \delta) \in U_1$, then the unique positive constant steady state $E^*(u^*, v^*)$ of system (3.1) is locally asymptotically stable.*

Furthermore, we have the following global stability result about $E^*(u^*, v^*)$.

Theorem 3.5. *Suppose that $\delta < \frac{\gamma}{\alpha+1}$ and $u^* \geq 1-\alpha$, then system (3.1) has a unique positive constant steady state E^*, which is globally stable.*

Proof. We define

$$E(u(x,t), v(x,t)) = \frac{\gamma}{\beta}\int_\Omega \int_{u^*}^{u} \frac{\Phi(\xi) - \Phi(u^*)}{\Phi(\xi)} d\xi dx + \int_\Omega \int_{v^*}^{v} \frac{\eta - v^*}{\eta} d\eta dx,$$

where $\Phi(u) = \frac{\beta u}{\alpha + u}$. Then

$$\begin{aligned} E_t(u, v) &= \frac{\gamma}{\beta}\int_\Omega \frac{\Phi(u) - \Phi(u^*)}{\Phi(u)} u_t dx + \int_\Omega \frac{v - v^*}{v} v_t dx \\ &= \int_\Omega \Big[\frac{\alpha\gamma(u-u^*)^2(1-\alpha-u-u^*)}{\beta(\alpha+u)(\alpha+u^*)} - (v-v^*)^2\Big] dx + I_2(t), \end{aligned}$$

where

$$\begin{aligned} I_2(t) &= \frac{d_1\gamma}{\beta}\int_\Omega \frac{\Phi(u) - \Phi(u^*)}{\Phi(u)} \Delta u dx + d_2\int_\Omega \frac{v - v^*}{v}\Delta v dx \\ &= -\Big[\frac{d_1\gamma}{\beta}\int_\Omega \frac{\Phi'(u)\Phi(u^*)}{\Phi^2(u)}|\nabla u|^2 dx + d_2\int_\Omega \frac{v^*}{v^2}|\nabla v|^2 dx\Big]. \end{aligned}$$

Notice that $\Phi'(u) > 0$ for $u \geq 0$. Thus, when $u^* \geq 1-\alpha$, $E_t \leq 0$ along an orbit $(u(x,t), v(x,t))$ of system (1.5) with positive initial value (u_0, v_0) and $E_t = 0$ only if $(u(x,t), v(x,t)) = (u^*, v^*)$. Therefore, we complete the proof. □

Remark 3.6. Our results in Theorem 3.5 improve the one in Du and Lou [11], where they showed that system (3.1) has a unique positive constant steady state E^*, which is globally attractive when $\delta < \frac{\gamma}{\alpha+1}$ and $\alpha \geq 1$. It is obvious that $u^* \geq 1-\alpha$ if $\alpha \geq 1$.

4. Codimension-1 bifurcations of reaction-diffusion system

In this section, we consider possible codimension-1 bifurcations around E^* of reaction-diffusion system (3.1), including Turing bifurcation and Hopf bifurcation.

4.1. Turing bifurcation

From Lemma 2.3, we know that the unique positive equilibrium $E^*(u^*, v^*)$ of local system (2.1) is locally asymptotically stable when $u^* \geq \frac{1-\alpha}{2}$, or $\frac{1-\alpha-\gamma}{2} < u^* < \frac{1-\alpha}{2}$ and $\delta < \delta_0$. From Theorem 3.4, we know that the unique positive constant steady state $E^*(u^*, v^*)$ of diffusive system (3.1) is locally asymptotically stable when $u^* \geq \frac{1-\alpha}{2}$. Next, we investigate Turing instability and Turing bifurcation around $E^*(u^*, v^*)$ of diffusive system (3.1) under the following conditions:

$$\frac{1-\alpha-\gamma}{2} < u^* < \frac{1-\alpha}{2}, \ \delta < \delta_0, \ (\alpha, \beta, \gamma, \delta) \in U_1, \tag{4.1}$$

where U_1 and δ_0 are given in (2.5) and (2.8), respectively.

Note that $\mathrm{Tr}_k(E^*) < 0$ for any $k \geq 0$ when $\frac{1-\alpha-\gamma}{2} < u^* < \frac{1-\alpha}{2}$ and $\delta < \delta_0$. Thus, we need to determine the region where $\varphi(\frac{k^2}{l^2}) = \mathrm{Det}_k(E^*) < 0$ and Turing instability may occur. If $\varphi(\frac{k^2}{l^2}) < 0$ for some k, then (3.9) has two real roots in which one is positive and another is negative, that is, Turing instability occurs.

A k-mode Turing bifurcation is referred to the characteristic equation $P_k(\lambda) = 0$ with a positive integer k having a zero root, while the other roots of $P_k = 0$ have non-zero real parts, and the corresponding transversal conditions hold, see Jiang et al. [25] for more details.

If $\overline{A} > d_1 \frac{1}{l^2}$, then we denote $\overline{k}$ as the largest positive integer such that

$$d_1 \frac{k^2}{l^2} < \overline{A}, \quad \text{for} \quad 0 < k \leq \overline{k}, \tag{4.2}$$

and define

$$d_2^k \triangleq \frac{\overline{A}\,\overline{D} - \overline{B}\,\overline{C} - d_1 \frac{k^2}{l^2} \overline{D}}{(\overline{A} - d_1 \frac{k^2}{l^2}) \frac{k^2}{l^2}}, \ 0 < k \leq \overline{k}. \tag{4.3}$$

Since

$$\frac{\mathrm{d}d_2^k}{\mathrm{d}k^2} = \frac{-\frac{d_1^2}{l^4} \overline{D} k^4 + 2(\overline{A}\,\overline{D} - \overline{B}\,\overline{C}) \frac{d_1}{l^2} k^2 - (\overline{A}\,\overline{D} - \overline{B}\,\overline{C}) \overline{A}}{\frac{k^4}{l^2} (\overline{A} - d_1 \frac{k^2}{l^2})^2},$$

we denote

$$k_0 \triangleq \left\lfloor \sqrt{\frac{\overline{B}\,\overline{C} - \overline{A}\,\overline{D} + \sqrt{\overline{B}\,\overline{C}(\overline{B}\,\overline{C} - \overline{A}\,\overline{D})}}{-\frac{d_1 \overline{D}}{l^2}}} \right\rfloor,$$

where $\lfloor \dot{} \rfloor$ is the floor function, then d_2^k monotonically decreases in interval $[1, k_0]$ if $k_0 > 1$, and monotonically increases in interval $[k_0 + 1, \overline{k}]$ if $k_0 + 1 < \overline{k}$. Denote

$$k_0^* = \begin{cases} \overline{k}, & k_0 \ge \overline{k}, \\ 1, & k_0 = 0, \\ k_0, & d_2^{k_0} < d_2^{k_0+1},\ 1 \le k_0 < \overline{k}, \\ k_0 + 1, & d_2^{k_0} > d_2^{k_0+1},\ 1 \le k_0 < \overline{k}. \end{cases} \tag{4.4}$$

Then for k_0^* given above, we have $d_2^{k_0^*} = \min\limits_{1 \le k \le \overline{k}} d_2^k$.

Let

$$\theta_2 = \frac{(\overline{A}\,\overline{D} - 2\overline{B}\,\overline{C}) + 2\sqrt{\overline{B}\,\overline{C}(\overline{B}\,\overline{C} - \overline{A}\,\overline{D})}}{\overline{A}^2}, \tag{4.5}$$

we have the following results about Turing instability and Turing bifurcation around $E^*(u^*, v^*)$ of diffusive system (3.1).

Theorem 4.1. *If the conditions in* (4.1) *hold, then we have*

(I) *when $d_2 < d_1\theta_2$, $E^*(u^*, v^*)$ is stable for system* (3.1)*;*
(II) *when $d_2 \ge d_1\theta_2$, and*
- **(i)** *if $d_1 \ge \overline{A}l^2$, or $d_1 < \overline{A}l^2$ and $d_2 < d_2^{k_0^*}$, then $E^*(u^*, v^*)$ is stable for system* (3.1)*;*
- **(ii)** *if $d_1 < \overline{A}l^2$ and $d_2 > d_2^{k_0^*}$, then $E^*(u^*, v^*)$ is unstable for system* (3.1)*, that is, Turing instability occurs;*
- **(iii)** *if $d_2 = d_2^{k_0^*}$, then system* (3.1) *undergoes k_0^*-mode Turing bifurcation around $E^*(u^*, v^*)$, where characteristic equations $P_k(\lambda) = 0$ have a zero eigenvalue with other eigenvalues having negative real parts.*

Proof. By (3.10), the necessary condition for $\varphi(\frac{k^2}{l^2}) < 0$ is $\overline{A}d_2 + d_1\overline{D} > 0$. Define the ratio $\theta = d_2/d_1$. Because $u^* < \frac{1-\alpha}{2}$, we have $\overline{A} > 0$, and

$$\overline{A}d_2 + d_1\overline{D} > 0 \Longleftrightarrow \theta > -\frac{\overline{D}}{\overline{A}} \triangleq \theta^*.$$

The discriminant of $\varphi(\frac{k^2}{l^2}) = 0$ is

$$\Lambda(d_1, d_2) = (\overline{A}d_2 + \overline{D}d_1)^2 - 4d_1d_2(\overline{A}\,\overline{D} - \overline{B}\,\overline{C}) = \overline{A}^2 d_2^2 + 2(2\overline{B}\,\overline{C} - \overline{A}\,\overline{D})d_1d_2 + \overline{D}^2 d_1^2.$$

Then

$$\Lambda(d_1, d_2) = 0 \Longleftrightarrow \overline{A}^2\theta^2 + 2(2\overline{B}\,\overline{C} - \overline{A}\,\overline{D})\theta + \overline{D}^2 = 0.$$

Since $\overline{B} < 0$, $\overline{C} > 0$, $\overline{D} < 0$ and $\overline{A}\,\overline{D} - \overline{B}\,\overline{C} > 0$, we have

$$4(2\overline{B}\,\overline{C} - \overline{A}\,\overline{D})^2 - 4\overline{A}^2\overline{D}^2 = 16\overline{B}\,\overline{C}(\overline{B}\,\overline{C} - \overline{A}\,\overline{D}) > 0.$$

Then $\Lambda(d_1, d_2) = 0$ has two positive real roots

$$\theta_{1,2} = \frac{(\overline{A}\,\overline{D} - 2\overline{B}\,\overline{C}) \pm 2\sqrt{\overline{B}\,\overline{C}(\overline{B}\,\overline{C} - \overline{A}\,\overline{D})}}{\overline{A}^2}.$$

Therefore,

$$\Lambda(d_1, d_2) > 0 \Longleftrightarrow \theta < \theta_1 \text{ or } \theta > \theta_2.$$

From

$$\theta_1 - \theta^* = \frac{2(\overline{A}\,\overline{D} - \overline{B}\,\overline{C}) - 2\sqrt{\overline{B}\,\overline{C}(\overline{B}\,\overline{C} - \overline{A}\,\overline{D})}}{\overline{A}^2},$$
$$\theta_2 - \theta^* = \frac{2(\overline{A}\,\overline{D} - \overline{B}\,\overline{C}) + 2\sqrt{\overline{B}\,\overline{C}(\overline{B}\,\overline{C} - \overline{A}\,\overline{D})}}{\overline{A}^2},$$

and

$$(\overline{A}\,\overline{D} - \overline{B}\,\overline{C})^2 - \overline{B}\,\overline{C}(\overline{B}\,\overline{C} - \overline{A}\,\overline{D}) = \overline{A}\,\overline{D}(\overline{A}\,\overline{D} - \overline{B}\,\overline{C}) < 0,$$

we have $0 < \theta_1 < \theta^* < \theta_2$. Therefore, the necessary condition for $\varphi(\frac{k^2}{l^2}) < 0$ is $\theta \geq \theta_2$, i.e., $d_2 \geq d_1\theta_2$.

Next we investigate the concrete region in $d_1 - d_2$ plane for $\varphi(\frac{k^2}{l^2}) < 0$. We rewrite $\varphi(\frac{k^2}{l^2})$ as

$$\varphi(\frac{k^2}{l^2}) = d_2\frac{k^2}{l^2}(d_1\frac{k^2}{l^2} - \overline{A}) + \overline{A}\,\overline{D} - \overline{B}\,\overline{C} - d_1\frac{k^2}{l^2}\overline{D}.$$

If $\overline{A} \leq d_1\frac{1}{l^2}$, then $\varphi(\frac{k^2}{l^2}) > 0$ for any $k \geq 1$, since $\overline{A}\,\overline{D} - \overline{B}\,\overline{C} > 0$ and $\overline{D} < 0$. This implies that E^* is stable.

If $\overline{A} > d_1\frac{1}{l^2}$ and $0 < d_2 < d_2^{k_0^*}$, where d_2^k and k_0^* are given in (4.3) and (4.4), respectively, then

$$\overline{A} > d_1\frac{k^2}{l^2} \quad \text{and} \quad d_2 < d_2^k, \quad k \in [1, \overline{k}],$$

which follows that $\varphi(\frac{k^2}{l^2}) > 0$ for all $k \in [1, \overline{k}]$. Furthermore, by the construction of $\overline{k}$ in (4.2), we know that $\overline{A} \leq d_1\frac{k^2}{l^2}$ and then $\varphi(\frac{k^2}{l^2}) > 0$ if $k > \overline{k}$. This means that $E^*(u^*, v^*)$ is stable.

If $\overline{A} > d_1\frac{1}{l^2}$ and $d_2 > d_2^{k_0^*}$, which implies that $\varphi(\frac{k_0^{*2}}{l^2}) < 0$ and then $E^*(u^*, v^*)$ is unstable.

Finally, when $d_2 = d_2^{k_0^*}$ and the conditions in (4.1) hold, we have $\mathrm{Det}_{k_0^*}(E^*) = 0$, $\mathrm{Tr}_{k_0^*}(E^*) < 0$, $\mathrm{Det}_k(E^*) > 0$ $(k \neq k_0^*)$, $\mathrm{Tr}_k(E^*) < 0$ $(k \neq k_0^*)$, and $\frac{\mathrm{dDet}_{k_0^*}(E^*)}{\mathrm{d}d_2}\Big|_{d_2=d_2^{k_0^*}} < 0$, thus system (3.1) undergoes k_0^*-mode Turing bifurcation around $E^*(u^*, v^*)$. $\square$

We denote the curves C_k and $C_{k_0^*}$ as

$$C_k : d_2 = d_2^k, \quad 0 < d_1 < \overline{A}l^2, \quad 0 < k \le \overline{k},$$
$$C_{k_0^*} : d_2 = d_2^{k_0^*},\ 0 < d_1 < \overline{A}l^2.$$

By simple analysis, the curves C_k, $k = 1, 2, \cdots$, are tangent to the line $d_2 = \theta_2 d_1$ (see Fig. 4.1(a)). According to Theorem 4.1, we can see that the region, where Turing instability and Turing pattern occur, lies on the left side of $d_1 = \overline{A}l^2$ and above $C_{k_0^*}$. And system (3.1) undergoes k_0^*-mode Turing bifurcation at curve $C_{k_0^*}$.

Remark 4.2. According to Theorem 4.1, we can see that $\theta^* > 1$ since $\delta < \delta_0$. Then, $d_2 > \theta_2 d_1 > \theta^* d_1 > d_1$, which implies that the predator must diffuse faster than the prey for the occurrence of diffusive instability in system (3.1). Moreover, we observe that the larger the space domain, i.e. l, the more likely the system undergoes Turing instability.

Next, we give some numerical simulations to illustrate the theoretical results. We fix $\alpha = \frac{3}{4}$, $\gamma = \frac{1}{4}$, $u^* = \frac{1}{16}$, $\delta = \frac{1}{208}$, and get $\beta = \beta^* = \frac{845}{16}$, $v^* = \frac{3}{208}$, $\theta_2 = \frac{717}{2} + 6\sqrt{3570} \approx 716.997$. In this case, the positive equilibrium $E^*(u^*, v^*)$ of ODE system (2.1) is locally asymptotically stable. Then we fix $l = 2$, $d_1 = 0.005$, we have $\overline{k} = 2$ since $\frac{\overline{A}l^2}{d_1} \approx 7.69231$, and have $k_0 = 1$, $\theta_2 d_1 \approx 3.58498$, $d_2^1 = \frac{11913}{1508} \approx 7.89987$, $d_2^2 = \frac{747}{208} \approx 3.59135$, which implies $k_0^* = 2$ and $d_2^{k_0^*} \approx 3.59135$. Eventually, we choose several values of d_2 in Fig. 4.1(b) and (c) to simulate the occurrence of Turing bifurcation for system (3.1) with the following three cases:

Case 1: if $d_2 = 1$, then $d_2 < \theta_2 d_1$, which implies the constant steady state $E^*(u^*, v^*)$ is stable for system (3.1) by Theorem 4.1**(I)**;

Case 2: if $d_2 = 3.59$, then $\theta_2 d_1 < d_2 < d_2^{k_0^*}$, which implies $E^*(u^*, v^*)$ is also stable for system (3.1) by Theorem 4.1**(II)(i)**;

Case 3: if $d_2 = 4$, then $d_2 > d_2^{k_0^*}$, which implies $E^*(u^*, v^*)$ is unstable and nonconstant steady states (Turing patterns) emerge for system (3.1) by Theorem 4.1**(II)(ii)**.

4.2. Hopf bifurcation

In this section, we consider Hopf bifurcation around $E^*(u^*, v^*)$. By Theorems 3.4 and 3.5, we assume $\frac{1}{2} \le \alpha < 1$, $0 < u^* < \frac{1-\alpha}{2}$. From Lemma 2.3, if $\frac{1-\alpha-\gamma}{2} < u^* < \frac{1-\alpha}{2}$ and $\delta < \delta_0$, then $\mathrm{Tr}_0 = \overline{A} + \overline{D} < 0$, thus $\mathrm{Tr}_k(E^*) = \mathrm{Tr}_0 - \frac{(d_1+d_2)k^2}{l^2} < 0$ for any $k \ge 0$. Hence, any potential Hopf bifurcation around E^* must satisfy $\frac{1}{2} \le \alpha < 1$, $\frac{1-\alpha-\gamma}{2} < u^* < \frac{1-\alpha}{2}$ and $\delta \ge \delta_0$, or $u^* \le \frac{1-\alpha-\gamma}{2}$.

According to Jiang et al. [25], a k-mode Hopf bifurcation is referred to the characteristic equation $P_k(\lambda) = 0$ with a nonnegative integer k having a pair of purely imaginary roots, while the other roots of $P_k(\lambda) = 0$ have non-zero real parts, and the corresponding transversal conditions hold.

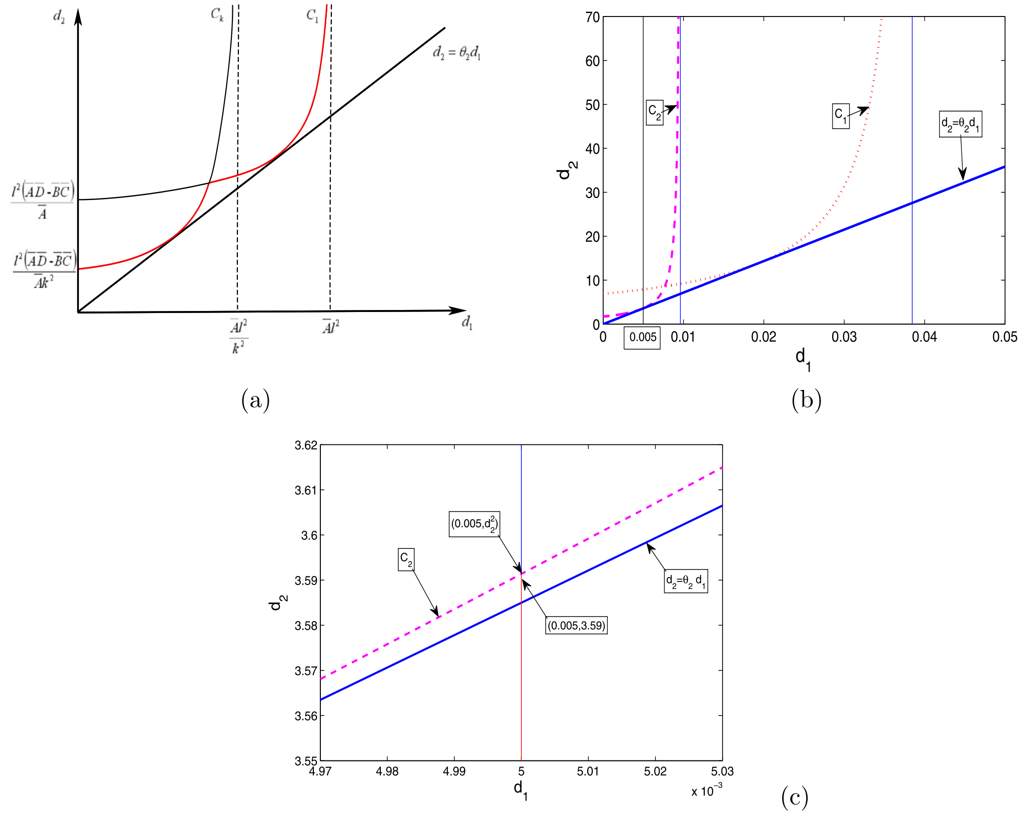

Fig. 4.1. (a) The region for Turing instability: (d_1, d_2) lies on the left side of $d_1 = \overline{A}l^2$ and above $C_{k_0^*}$ (the red curve); (b) The curves C_1, C_2, the line $d_2 = \theta_2 d_1$, the vertical lines $d_1 = \overline{A}l^2$ and $d_1 = \overline{A}l^2/4$ (thin blue vertical lines from right) when $\alpha = \frac{3}{4}, \gamma = \frac{1}{4}, \delta = \frac{1}{208}, \beta = \frac{845}{16}, u^* = \frac{1}{16}, v^* = \frac{3}{208}, l = 2$; (c) The local enlarged view of (b) at $(0.005, 3.59)$. (For interpretation of the colors in the figure(s), the reader is referred to the web version of this article.)

Theorem 4.3. *Assume* $\alpha < 1$, $\frac{1-\alpha-\gamma}{2} < u^* < \frac{1-\alpha}{2}$, $(\alpha, \beta, \gamma, \delta) \in U_1$, *and one of the following conditions holds:*

(I) $d_2 < d_1\theta_2$;
(II) $d_2 \geq d_1\theta_2$ *and* $d_1 \geq \overline{A}l^2$;
(III) $d_2 \geq d_1\theta_2$, $d_1 < \overline{A}l^2$ *and* $d_2 < d_2^{k_0^*}$.

System (3.1) *undergoes* 0*-mode Hopf bifurcation (i.e., spatially homogeneous Hopf bifurcation) around* E^* *at* $\delta = \delta_0$*, where the characteristic equation* $P_0(\lambda) = 0$ *has a pair of purely imaginary roots, while the other roots of* $P_k(\lambda) = 0$ $(k > 0)$ *have negative real parts. Where* θ_2, $d_2^{k_0^*}$, k_0^* *are defined in* (4.5), (4.3) *and* (4.4)*, respectively.*

Proof. Since $\frac{\mathrm{dTr}_0(E^*)}{\mathrm{d}\delta} = 1$, then $\mathrm{Tr}_0(E^*) = 0$ has a unique root $\delta = \delta_0$, and clearly the corresponding transversal conditions hold. In addition, it is easy to see $\mathrm{Tr}_j(E^*)(\delta_0) < 0$ $(j \geq 1)$. Clearly, $\mathrm{Det}_0(E^*) = \mathrm{Det}_0 > 0$. According to the proof of Theorem 4.1, we have $\mathrm{Det}_k(E^*) >$

0 $(k \geq 1)$ if one of conditions **(I)**, **(II)** and **(III)** holds. Thus system (3.1) undergoes 0-mode Hopf bifurcation. □

Next we seek spatially inhomogeneous Hopf bifurcation for $k \geq 1$. Notice that $\overline{A} + \overline{D}$ monotonically increase in δ, then $0 < \overline{A} + \overline{D} = \delta - \delta_0 < \overline{A}$ for $\delta_0 < \delta < \frac{\gamma u^*}{\alpha + u^*}$. If $(d_1 + d_2)\frac{1}{l^2} < \overline{A}$, then we define $\hat{k}$ to be the largest positive integer such that

$$(d_1 + d_2)\frac{k^2}{l^2} < \overline{A}, \quad \text{for} \quad 1 \leq k \leq \hat{k}, \tag{4.6}$$

and define

$$\delta_k^H = \delta_0 + \frac{(d_1 + d_2)k^2}{l^2} \quad \text{for} \quad 1 \leq k \leq \hat{k} \tag{4.7}$$

to be the roots of $\mathrm{Tr}_k(E^*) = \delta - \delta_0 - (d_1 + d_2)\frac{k^2}{l^2} = 0$. We have the following results.

Theorem 4.4. *Assume $\alpha < 1$, $0 < u^* < \frac{1-\alpha}{2}$, $\delta > \delta_0$, $(\alpha, \beta, \gamma, \delta) \in U_1$, and one of the following conditions holds:*

- **(I)** $d_2 < d_1\theta_2$*;*
- **(II)** $d_2 \geq d_1\theta_2$ *and* $d_1 \geq \overline{A}l^2$*;*
- **(III)** $d_2 \geq d_1\theta_2$*,* $d_1 < \overline{A}l^2$ *and* $d_2 < d_2^{k_0^*}$*.*

If $d_2 < \overline{A}l^2 - d_1$, then system (3.1) undergoes k-mode Hopf bifurcation around E^* at $\delta = \delta_k^H$ for $k \in [1, \hat{k}]$, where the characteristic equation $P_k(\lambda) = 0$ with a positive integer k having a pair of purely imaginary roots, $2k$ positive real roots, while the other roots of $P_j(\lambda) = 0$ $(j > k)$ have negative real parts. Where θ_2, d_2^k, k_0^* are defined in (4.5), (4.3) and (4.4), respectively.

Proof. To seek spatially inhomogeneous Hopf bifurcation points for $k \geq 1$, we need to find the roots of $\overline{A} + \overline{D} = (d_1 + d_2)\frac{k^2}{l^2}$. If $(d_1 + d_2)\frac{1}{l^2} \geq \overline{A}$, then $(d_1 + d_2)\frac{k^2}{l^2} \geq \overline{A}$ for any $k = 1, 2, \cdots$. It follows that $\overline{A} + \overline{D} \neq (d_1 + d_2)\frac{k^2}{l^2}$, for any $k = 1, 2, \cdots$. If $(d_1 + d_2)\frac{1}{l^2} < \overline{A}$, then we have $(d_1 + d_2)\frac{k^2}{l^2} > \overline{A}$ for $k \in (\hat{k}, \infty)$ from (4.6), which implies $\overline{A} + \overline{D} \neq (d_1 + d_2)\frac{k^2}{l^2}$, for $k > \hat{k}$.

Since $\frac{\mathrm{dTr}_k(E^*)}{\mathrm{d}\delta} = 1$, it is easy to see that $\mathrm{Tr}_k(E^*) = 0$ has a unique root $\delta = \delta_k^H$ for $k \in [1, \hat{k}]$, and clearly the corresponding transversal conditions hold. In addition, it is easy to see that $\mathrm{Tr}_j(E^*)(\delta_k^H) > 0$ for $j < k$, and $\mathrm{Tr}_j(E^*)(\delta_k^H) < 0$ for $j > k$. According to the proof of Theorem 4.1, we have $\mathrm{Det}_k(E^*) > 0$ for any $k \geq 0$ if one of conditions **(I)**, **(II)** and **(III)** is satisfied. Thus system (3.1) undergoes k-mode Hopf bifurcation. □

Next we consider the bifurcation direction and stability of the bifurcating periodic solutions by applying the normal form theory and center manifold theorem introduced by Hassard et al. [24].

We introduce the translation $\hat{u} = u - u^*$ and $\hat{v} = v - v^*$, then system (3.1) becomes (still denote $\hat{u}$ and $\hat{v}$ as u and v, respectively)

$$\begin{cases} u_t - d_1 u_{xx} = (u+u^*)(1-u-u^*) - \dfrac{\beta^*(u+u^*)(v+v^*)}{\alpha+u+u^*}, & x \in (0, l\pi),\ t>0, \\ v_t - d_2 v_{xx} = -\delta(v+v^*) + \dfrac{\gamma(u+u^*)(v+v^*)}{\alpha+u+u^*} - (v+v^*)^2, & x \in (0, l\pi),\ t>0, \\ u_x(0,t) = v_x(0,t) = 0,\ u_x(l\pi,t) = v_x(l\pi,t) = 0, & t>0. \end{cases} \tag{4.8}$$

Rewrite system (4.8) as

$$\begin{pmatrix} u_t \\ v_t \end{pmatrix} = \hat{D} \begin{pmatrix} u_{xx} \\ v_{xx} \end{pmatrix} + J(E^*) \begin{pmatrix} u \\ v \end{pmatrix} + \begin{pmatrix} f_1(u,v,\delta) \\ g_1(u,v,\delta) \end{pmatrix}, \tag{4.9}$$

where

$$f_1(u,v,\delta) = a_{20}u^2 + a_{11}uv + a_{30}u^3 + a_{21}u^2v + o(|(u,v)|^3),$$
$$g_1(u,v,\delta) = b_{20}u^2 + b_{11}uv + b_{02}v^2 + b_{30}u^3 + b_{21}u^2v + o(|(u,v)|^3),$$

and

$$a_{20} = -2 + \frac{2(1-u^*)\alpha}{(u^*+\alpha)^2}, \quad a_{11} = -\frac{2\alpha\beta}{(u^*+\alpha)^2}, \quad a_{30} = -\frac{6\alpha(1-u^*)}{(u^*+\alpha)^3}, \quad a_{21} = \frac{6\alpha\beta}{(u^*+\alpha)^3},$$
$$b_{20} = -\frac{2(1-u^*)\alpha\gamma}{(u^*+\alpha)^2\beta}, \quad b_{11} = \frac{2\alpha\gamma}{(u^*+\alpha)^2}, \quad b_{02} = -2, \quad b_{30} = \frac{6\alpha(1-u^*)\alpha\gamma}{(u^*+\alpha)^3\beta},$$
$$b_{21} = -\frac{6\alpha\gamma}{(u^*+\alpha)^3}.$$

Let

$$\mathrm{Re}(c_1(\delta_0)) = \frac{u^*\sigma_{11}}{2(\alpha+u^*)^5 \mathrm{Det}_0}, \tag{4.10}$$

where σ_{11} and Det_0 are given in (2.9) and (2.8), respectively. We have the following results.

Theorem 4.5. *If the conditions in Theorem 4.3 hold, then system (3.1) undergoes 0-mode Hopf bifurcation around E^* at $\delta = \delta_0$. Moreover,*

(i) *if $\sigma_{11} < 0$, then the Hopf bifurcation is supercritical, and the bifurcating (spatially homogeneous) periodic solutions are orbitally asymptotically stable when $\delta > \delta_0$.*
(ii) *if $\sigma_{11} > 0$, then the Hopf bifurcation is subcritical, and the bifurcating (spatially homogeneous) periodic solutions are unstable $\delta < \delta_0$.*

Proof. When $\delta = \delta_0$, then $P_0(\lambda) = 0$ has a pair of purely imaginary eigenvalues $\pm i\omega_0 = \pm i\sqrt{\mathrm{Det}_0}$, where Det_0 is defined in (2.8).

For any $\xi_i = (\xi_{i1}, \xi_{i2})^\top \in X_{\mathbb{C}}$ $(i = 1, 2)$, let $\langle \xi_1, \xi_2 \rangle$ be the complex-valued L^2 inner product on Hilbert space $X_{\mathbb{C}}$, defined as

$$\langle \xi_1, \xi_2 \rangle = \int_0^{l\pi} (\overline{\xi}_{11}\xi_{21} + \overline{\xi}_{12}\xi_{22}) dx.$$

Denote L^* be the conjugate operator of L such that $\langle \xi_1, L\xi_2 \rangle = \langle L^*\xi_1, \xi_2 \rangle$:

$$L^* \begin{pmatrix} u \\ v \end{pmatrix} = \hat{D} \begin{pmatrix} u_{xx} \\ v_{xx} \end{pmatrix} + (J(E^*))^\top \begin{pmatrix} u \\ v \end{pmatrix} \tag{4.11}$$

with the domain $D_L^* = X_{\mathbb{C}}$. We choose $q \in X_{\mathbb{C}}$ such that $L(\delta_0)q = i\omega_0 q$. Thus, we have

$$q = \begin{pmatrix} q_1 \\ q_2 \end{pmatrix} = \begin{pmatrix} 1 \\ \frac{i\omega_0 - \overline{A}}{\overline{B}} \end{pmatrix}. \tag{4.12}$$

Then, we choose $q^* \in X_{\mathbb{C}}$ so that

$$L^*(\delta_0)q^* = -i\omega_0 q^*, \quad \langle q^*, q \rangle = 1 \quad \text{and} \quad \langle q^*, \overline{q} \rangle = 0.$$

Thus,

$$q^* = \begin{pmatrix} q_1^* \\ q_2^* \end{pmatrix} = \frac{1}{2l\pi\omega_0} \begin{pmatrix} \omega_0 + i\overline{A} \\ i\overline{B} \end{pmatrix}. \tag{4.13}$$

By Hassard et al. [24] (see also [56]), we have

$$Q_{qq} := (c_0, d_0)^\top, \quad Q_{q\overline{q}} := (e_0, f_0)^\top, \quad C_{qq\overline{q}} := (g_0, h_0)^\top,$$

where

$$\begin{aligned} &c_0 := 2a_{20} + 2a_{11}q_2, \quad d_0 := 2b_{20} + 2b_{11}q_2 + 2b_{02}q_2^2, \quad e_0 := 2a_{20} + a_{11}(q_2 + \overline{q_2}), \\ &f_0 := 2b_{20} + b_{11}(q_2 + \overline{q_2}) + 2b_{02}|q_2|^2, \quad g_0 := 6a_{30} + 2a_{21}(2q_2 + \overline{q_2}), \\ &h_0 := 6b_{30} + 2b_{21}(2q_2 + \overline{q_2}). \end{aligned}$$

Since

$$\begin{aligned} &\langle q^*, Q_{qq} \rangle = (\overline{q_1^*}c_0 + \overline{q_2^*}d_0)l\pi, \quad \langle \overline{q^*}, Q_{qq} \rangle = (q_1^*c_0 + q_2^*d_0)l\pi, \quad \langle q^*, Q_{q\overline{q}} \rangle = (\overline{q_1^*}e_0 + \overline{q_2^*}f_0)l\pi, \\ &\langle \overline{q^*}, Q_{q\overline{q}} \rangle = (q_1^*e_0 + q_2^*f_0)l\pi, \quad \langle q^*, C_{qq\overline{q}} \rangle = (\overline{q_1^*}g_0 + \overline{q_2^*}h_0)l\pi. \end{aligned}$$

It is straightforward to calculate

$$H_{20} = Q_{qq} - \langle q^*, Q_{qq} \rangle q - \langle \overline{q^*}, Q_{qq} \rangle \overline{q} = 0, \quad H_{11} = Q_{q\overline{q}} - \langle q^*, Q_{q\overline{q}} \rangle q - \langle \overline{q^*}, Q_{q\overline{q}} \rangle \overline{q} = 0,$$

which implies that

$$w_{20} = [2i\omega_0 I - L(\delta_0)]^{-1} H_{20} = 0, \quad w_{11} = -[L(\delta_0)]^{-1} H_{11} = 0.$$

Thus, we have

$$\langle q^*, Q_{w_{11}q}\rangle = \langle q^*, Q_{w_{20}\overline{q}}\rangle = 0,$$

where

$$Q_{w_{11}q} = (2a_{20}q_1 + a_{11}q_2,\ a_{11}q_1)w_{11}, \quad Q_{w_{20}\overline{q}} = (2a_{20}\overline{q_1} + a_{11}\overline{q_2},\ a_{11}\overline{q_1})w_{20}.$$

Finally, the reaction-diffusion system restricted to the center manifold is given by

$$\frac{dz}{dt} = i\omega_0 z + \sum_{2\le i+j\le 3} \frac{g_{ij}}{i!j!} z^i \overline{z}^j + o(|z|^3), \tag{4.14}$$

where

$$g_{20} = \langle q^*, Q_{qq}\rangle, \quad g_{11} = \langle q^*, Q_{q\overline{q}}\rangle, \quad g_{02} = \langle q^*, Q_{\overline{q}\overline{q}}\rangle, \quad g_{21} = \langle q^*, C_{qq\overline{q}}\rangle.$$

According to Hassard et al. [24], we have

$$c_1(\delta_0) = \frac{i}{2\omega_0}\left(g_{20}g_{11} - 2|g_{11}|^2 - \frac{1}{3}|g_{02}|^2\right) + \frac{g_{21}}{2}, \tag{4.15}$$

and

$$\begin{aligned} \mathrm{Re}(c_1(\delta_0)) &= -\frac{1}{2\omega_0}\Big[\mathrm{Re}(g_{20})\mathrm{Im}(g_{11}) + \mathrm{Im}(g_{20})\mathrm{Re}(g_{11})\Big] + \frac{\mathrm{Re}(g_{21})}{2} \\ &= \frac{u^*\sigma_{11}}{2(\alpha+u^*)^5\mathrm{Det}_0}, \end{aligned} \tag{4.16}$$

where we have eliminated β by $\beta = \beta^*$, and Det_0, σ_{11} are given in (2.7) and (2.9), respectively. □

Remark 4.6. Comparing (2.9) with (4.10), we can find that the sign of $\mathrm{Re}(c_1(\delta_0))$ for system (3.1) is the same as σ_{11}, i.e., as σ_1 for system (2.1). Therefore, the stability and direction of Hopf bifurcation of diffusive system (3.1) is same as that of corresponding local system (2.1).

5. Codimension-2 bifurcations of reaction-diffusion system (3.1)

In this section, we consider possible codimension-2 bifurcations of reaction-diffusion system (3.1) at $E^*(u^*, v^*)$, including Turing-Turing bifurcation (spatial resonance bifurcation) and Turing-Hopf bifurcation.

5.1. Turing-Turing bifurcation

From section 3, we know that system (3.1) may undergo Turing-Turing bifurcation at $E^*(u^*, v^*)$, which is degenerate Turing bifurcation. Let

$$d_1^{i,j} = \frac{(i^2+j^2)(\overline{A}\,\overline{D}-\overline{B}\,\overline{C})+\sqrt{(i^2+j^2)^2(\overline{A}\,\overline{D}-\overline{B}\,\overline{C})^2-4i^2j^2\overline{A}\,\overline{D}(\overline{A}\,\overline{D}-\overline{B}\,\overline{C})}}{2\overline{D}i^2j^2},$$

$$d_2^{i,j} = \frac{\overline{A}\,\overline{D}-\overline{B}\,\overline{C}-d_1^{i,j}\frac{i^2}{l^2}\overline{D}}{(\overline{A}-d_1^{i,j}\frac{i^2}{l^2})\frac{i^2}{l^2}}, \quad i, j \in [1, \overline{k}].$$

Then, we have following theorem of Turing-Turing bifurcation.

Theorem 5.1. *If $\frac{1-\alpha-\gamma}{2} < u^* < \frac{1-\alpha}{2}$, $\delta < \delta_0$ and $(\alpha, \beta, \gamma, \delta) \in U_1$ hold, then system (3.1) undergoes a (i, j)-mode Turing-Turing bifurcation at $E^*(u^*, v^*)$ when $(d_1, d_2) = (d_1^{i,j}, d_2^{i,j})$, $i, j \in [1, \overline{k}]$, where characteristic equations $P_k(\lambda) = 0$ have two independent zero eigenvalues, while other roots of $P_k(\lambda) = 0$ having non-zero real parts. Moreover, system (3.1) can not exhibit triple-Turing bifurcation at $E^*(u^*, v^*)$.*

Proof. Turing-Turing bifurcation point is the intersection point of two Turing bifurcation curves C_k with different wavelengths, see [45,53]. We will prove this theorem in three steps.

(I) For $i, j \in \mathbb{N}$ and $i, j \in [1, \overline{k}]$, let $j > i$, then Turing curve C_j intersects with curve C_i in the first quadrant in $d_1 - d_2$ plane.

We have

$$\lim_{d_1 \to 0^+} d_2^k = \frac{l^2(\overline{A}\,\overline{D}-\overline{B}\,\overline{C})}{\overline{A}k^2} > 0,$$

which implies $\lim\limits_{d_1 \to 0^+} d_2^k$ monotonically decreases in k. Thus there exists a sufficiently small $\epsilon > 0$ satisfying that $d_2^k(\epsilon)$ monotonically decreases in k, i.e., $d_2^j(\epsilon) < d_2^i(\epsilon)$. Moreover,

$$\lim_{d_1 \to (\frac{\overline{A}l^2}{j^2})^-} d_2^j = +\infty, \quad d_2^i(\frac{\overline{A}l^2}{j^2}) = \frac{l^2(\overline{A}\,\overline{D}-\overline{B}\,\overline{C}-\overline{A}\,\overline{D}\frac{i^2}{j^2})}{\overline{A}i^2(1-\frac{i^2}{j^2})} < +\infty.$$

Therefore, by the continuity of d_2^k in d_1, we have $d_2^j(\frac{\overline{A}l^2}{j^2}-\epsilon_1) - d_2^i(\frac{\overline{A}l^2}{j^2}-\epsilon_1) > 0$ for sufficiently small $\epsilon_1 > 0$. We define function $d(d_1) = d_2^j(d_1) - d_2^i(d_1)$ with $d_1 \in [\epsilon, \frac{\overline{A}l^2}{j^2}-\epsilon_1]$, then $d(\epsilon) < 0$ and $d(\frac{\overline{A}l^2}{j^2}-\epsilon_1) > 0$. Thus, there exists a $d_1^{i,j}$ satisfying $d(d_1^{i,j}) = 0$, i.e., $d_2^j(d_1^{i,j}) = d_2^i(d_1^{i,j})$.

(II) C_j and C_i only intersect at one point.

By direct computation, we have

$$\frac{\mathrm{d}d_2^k}{\mathrm{d}d_1} = \frac{-\overline{B}\,\overline{C}}{(\overline{A}-d_1\frac{k^2}{l^2})^2} > 0.$$

Denote $ll_k = \frac{\mathrm{d}d_2^k}{\mathrm{d}d_1}$, then

$$\frac{\mathrm{d}ll_k}{\mathrm{d}d_1} = \frac{-2\overline{B}\,\overline{C}k^2}{l^2(\overline{A} - d_1\frac{k^2}{l^2})^3} > 0, \quad \frac{\mathrm{d}ll_k}{\mathrm{d}k} = \frac{-4\overline{B}\,\overline{C}d_1 k}{l^2(\overline{A} - d_1\frac{k^2}{l^2})^3} > 0.$$

Thus, $d_2 = d_2^k$ i.e., C_k monotonically increases in d_1, and ll_k monotonically increases in d_1 and in k, see Fig. (4.1)(a). From the property of C_k, we reach the conclusions. In fact, if there is another intersection point $(d_1^{i,j,1}, d_2^{i,j,1})$ of C_j and C_i, we have

$$d_2^{i,j,1} - d_2^{i,j} = \int_{d_1^{i,j}}^{d_1^{i,j,1}} ll_i \mathrm{d}d_1 = \int_{d_1^{i,j}}^{d_1^{i,j,1}} ll_j \mathrm{d}d_1,$$

which is obviously a contradiction, since $ll_i < ll_j$ for all $d_1 \in (d_1^{i,j}, d_1^{i,j,1})$.

Therefore, we denote the unique intersection between C_i and C_j by $(d_1^{i,j}, d_2^{i,j})$, and $d_1^{i,j}$ satisfies the following equation:

$$i^2 j^2 \frac{\overline{D}}{l^4} d_1^2 - (i^2 + j^2)\frac{\overline{A}\,\overline{D} - \overline{B}\,\overline{C}}{l^2} d_1 + \overline{A}(\overline{A}\,\overline{D} - \overline{B}\,\overline{C}) = 0.$$

Thus, by solving the above equation directly, we obtain a positive root

$$d_1^{i,j} = \frac{(i^2 + j^2)(\overline{A}\,\overline{D} - \overline{B}\,\overline{C}) + \sqrt{(i^2 + j^2)^2(\overline{A}\,\overline{D} - \overline{B}\,\overline{C})^2 - 4i^2 j^2 \overline{A}\,\overline{D}(\overline{A}\,\overline{D} - \overline{B}\,\overline{C})}}{2\overline{D}i^2 j^2} > 0.$$

Then substituting $d_1^{i,j}$ into d_2^i, we obtain $d_2^{i,j}$.

(III) If $i < j < k$, then C_i, C_j and C_k will not intersect at the same point.

By simple analysis, we can see that the curve C_k $(k = 1, 2, \cdots, \overline{k})$ is tangent to $d_2 = \theta_2 d_1$ at a unique point $(d_{1k}, \theta_2 d_{1k})$, where

$$d_{1k} = \frac{l^2\overline{A}\left(\overline{A}\,\overline{D} - \overline{B}\,\overline{C} + \sqrt{\overline{B}\,\overline{C}(\overline{B}\,\overline{C} - \overline{A}\,\overline{D})}\right)}{k^2\left(\overline{A}\,\overline{D} - 2\overline{B}\,\overline{C} + 2\sqrt{\overline{B}\,\overline{C}(\overline{B}\,\overline{C} - \overline{A}\,\overline{D})}\right)},$$

and d_{1k} monotonically decreases in k, and $d_2^k > \theta_2 d_1$ $(d_1 \neq d_{1k})$ for $k = 1, 2, \cdots, \overline{k}$. Moreover, combining the proof of step **(I)** and **(II)**, we obtain that the unique intersection point $(d_1^{i,j}, d_2^{i,j})$ of C_i and C_j $(i < j)$ satisfies $d_1^{i,j} \in (d_{1j}, d_{1i})$. Thus, C_i, C_j and C_k $(i < j < k)$ will not intersect at the same point.

When $d_1 = d_1^{i,j}$, $d_2 = d_2^{i,j}$, $\mathrm{Det}_i(E^*) = \mathrm{Det}_j(E^*) = 0$, $\mathrm{Det}_k(E^*) \neq 0$ $(k \neq i, j)$, $\mathrm{Tr}_k(E^*) < 0$ $(k \geq 0)$, and $\frac{\mathrm{dDet}_k(E^*)}{\mathrm{d}d_2} \neq 0$ $(k = i, j)$ since $\frac{1-\alpha-\gamma}{2} < u^* < \frac{1-\alpha}{2}$, $\delta < \delta_0$ and $(\alpha, \beta, \gamma, \delta) \in U_1$. Thus, system (3.1) undergoes (i, j)-mode Turing-Turing bifurcation at $(d_1^{i,j}, d_2^{i,j})$. Moreover, the proof of step **(III)** implies, system (3.1) cannot exhibit triple-Turing bifurcation at $E^*(u^*, v^*)$, where characteristic equations $P_k(\lambda)=0$ have three independent zero eigenvalues with other eigenvalues having non-zero real parts. □

Finally, we explore some special Turing-Turing bifurcation points, where $P_k(\lambda)=0$ have two independent zero eigenvalues with other eigenvalues having negative real parts. From the proof in Theorems 4.1 and 5.1, we obtain that the unique intersection point $(d_1^{i,j}, d_2^{i,j})$ of C_i and C_j $(i<j)$ satisfies $d_2^{i,j}$ monotonically decreases in i and $d_2^{j-1,j} = \min\limits_{1\le i\le j-1} d_2^{i,j}$. Thus, we have the following results.

Theorem 5.2. *If $\frac{1-\alpha-\gamma}{2} < u^* < \frac{1-\alpha}{2}$, $\delta<\delta_0$ and $(\alpha,\beta,\gamma,\delta)\in U_1$, then system (3.1) undergoes a $(k-1,k)$-mode Turing-Turing bifurcation, i.e., spatial resonance bifurcation, at $E^*(u^*,v^*)$ when $(d_1,d_2)=(d_1^{k-1,k}, d_2^{k-1,k})$, $k\in(1,\overline{k}]$.*

5.2. Turing-Hopf bifurcation

In this section, we consider the existence of Turing-Hopf bifurcation in system (3.1) under the condition U_1.

If there exist a positive integer k_1 and a nonnegative integer k_2 ($k_2\ne k_1$) such that $P_{k_1}(\lambda)=0$ has a simple zero root and $P_{k_2}(\lambda)=0$ has a pair of purely imaginary roots, while all other eigenvalues of $P_k(\lambda)=0$ have non-zero real parts, and the corresponding transversal conditions hold, then we call that a (k_1,k_2)-mode Turing-Hopf bifurcation occurs, see Jiang et al. [25] for details.

Theorem 5.3. *Assume $\alpha<1$, $\frac{1-\alpha-\gamma}{2} < u^* < \frac{1-\alpha}{2}$ and $(\alpha,\beta,\gamma,\delta)\in U_1$, system (3.1) exhibits $(k,0)$-mode Turing-Hopf bifurcation at $E^*(u^*,v^*)$ when $(d_2,\delta)=(d_2^k,\delta_0)$ and $d_1<\frac{\overline{A}l^2}{k^2}$ ($k\in[1,\overline{k}]$). Moreover, when $(d_2,\delta)=(d_2^{k_0^*},\delta_0)$ and $d_1<\overline{A}l^2$, system (3.1) undergoes a $(k_0^*,0)$-mode Turing-Hopf bifurcation, where all other eigenvalues of $P_k(\lambda)=0$ have negative real parts besides a simple zero eigenvalue and a pair of pure imaginary eigenvalues.*

Proof. From Theorems 4.1 and 4.3, we know that Turing bifurcation curves $C_{k_0^*}$ and Hopf bifurcation curve $\delta=\delta_0$ intersect at $(d_2,\delta)=(d_2^{k_0^*},\delta_0)$, if $\alpha<1$, $\frac{1-\alpha-\gamma}{2}<u^*<\frac{1-\alpha}{2}$, $d_1<\frac{\overline{A}l^2}{k^2}$. Clearly, $\mathrm{Tr}_0(E^*)=0$, $\mathrm{Det}_0(E^*)>0$, $\mathrm{Tr}_{k_0^*}(E^*)<0$ and $\mathrm{Det}_{k_0^*}(E^*)=0$ at $(d_2,\delta)=(d_2^{k_0^*},\delta_0)$. In addition, we have $\mathrm{Tr}_k(E^*)<0$ at $(d_2,\delta)=(d_2^{k_0^*},\delta_0)$ for any $k\ne 0$. And $\mathrm{Det}_k(E^*)>0$ at $(d_2,\delta)=(d_2^{k_0^*},\delta_0)$, for any $k\ne k_0^*$, since $d_2^{k_0^*}=\min\limits_{1\le k\le \overline{k}} d_2^k$. This implies the real parts of the eigenvalues of $P_k(\lambda)=0$ ($k\ne 0,\ k_0^*$) are all negative. Moreover, supposing $\lambda_1=\kappa_1+i\nu_1$ and $\lambda_2=\kappa_2+i\nu_2$, where $\kappa_1=0$, $\nu_1=\omega_0$, $\kappa_2=0$ and $\nu_2=0$ when $(d_2,\delta)=(d_2^{k_0^*},\delta_0)$, then we have the transversality conditions:

$$\frac{\mathrm{d}\kappa_1}{\mathrm{d}\delta}\Big|_{\delta=\delta_0}=\frac{1}{2}>0,$$

$$\frac{\mathrm{d}\kappa_2}{\mathrm{d}d_2}\Big|_{d_2=d_2^{k_0^*}}=\frac{\frac{k_0^{*2}}{l^2}\left(d_1\frac{k_0^{*2}}{l^2}-\overline{A}\right)}{\mathrm{Tr}_{k_0^*}(E^*)}>0,\quad \text{for}\quad \delta\le\delta_0.$$

The proof is completed. □

Next, we calculate the normal forms of $(k_0^*, 0)$-mode Turing-Hopf bifurcation for reaction-diffusion system (3.1) at $E^*(u^*, v^*)$.

We choose d_2 and δ as bifurcation parameters, and let $d_2 = d_2^{k_0^*} + \mu_1,\ \delta = \delta_0 + \mu_2$, and obtain the unfolding system from system (3.1) as follows:

$$\begin{cases} u_t - d_1 u_{xx} = u(1-u) - \dfrac{\beta u v}{\alpha + u}, & x \in (0, l\pi),\ t > 0, \\ v_t - (d_2^{k_0^*} + \mu_1) v_{xx} = -(\delta_0 + \mu_2) v + \dfrac{\gamma u v}{\alpha + u} - v^2, & x \in (0, l\pi),\ t > 0. \end{cases} \tag{5.1}$$

The constant steady state of system (5.1) is $E^*(u^*, v^*)$, where u^* satisfies $F(u^*) = 0$ and $v^* = -\delta_0 - \mu_2 + \frac{\gamma u^*}{\alpha + u^*}$. To apply the generic formulas developed by Jiang et al. [25] directly, we consider the transformation $\overline{u} = u - u^*$, $\overline{v} = v - v^*$, then system (5.1) is transformed into (still denote $\overline{u}$ and $\overline{v}$ by u and v, respectively)

$$\begin{cases} u_t - d_1 u_{xx} = (u + u^*)(1 - u - u^*) - \dfrac{\beta (u + u^*)(v + v^*)}{\alpha + u + u^*}, \\ v_t - (d_2^{k_0^*} + \mu_1) v_{xx} = -(\delta_0 + \mu_2)(v + v^*) + \dfrac{\gamma (u + u^*)(v + v^*)}{\alpha + u + u^*} - (v + v^*)^2. \end{cases} \tag{5.2}$$

According to [25], for system (5.2), we have

$$D(\mu) = \begin{pmatrix} d_1 & 0 \\ 0 & d_2^{k_0^*} + \mu_1 \end{pmatrix}, \quad L(\mu) = \begin{pmatrix} \overline{A} & \overline{B} \\ \overline{C} & -\overline{A} + \mu_2 \end{pmatrix},$$

$$F(\xi, \mu) = \begin{pmatrix} (\xi_1 + u^*)(1 - \xi_1 - u^*) - \frac{\beta(\xi_1 + u^*)(\xi_2 + v^*)}{\alpha + \xi_1 + u^*} - \overline{A}\xi_1 - \overline{B}\xi_2 \\ -(\delta_0 + \mu_2)(\xi_2 + v^*) + \frac{\gamma(\xi_1 + u^*)(\xi_2 + v^*)}{\alpha + \xi_1 + u^*} - (\xi_2 + v^*)^2 - \overline{C}\xi_1 - (-\overline{A} + \mu_2)\xi_2 \end{pmatrix},$$

where $\xi = (\xi_1, \xi_2)^T \in X$.

Then we attain

$$D_0(\mu) = \begin{pmatrix} d_1 & 0 \\ 0 & d_2^{k_0^*} \end{pmatrix}, \quad D_1(\mu) = \begin{pmatrix} 0 & 0 \\ 0 & 2\mu_1 \end{pmatrix},$$

$$L_0(\mu) = \begin{pmatrix} \overline{A} & \overline{B} \\ \overline{C} & -\overline{A} \end{pmatrix}, \quad L_1(\mu) = \begin{pmatrix} 0 & 0 \\ 0 & 2\mu_2 \end{pmatrix},$$

where $D_0(\mu) = D(0)$, $L_0(\mu) = L(0)$, $D_1(\mu)$ and $L_1(\mu)$ satisfy

$$D(\mu) = D(0) + \frac{1}{2} D_1(\mu) + \cdots, \quad L(\mu)u = L(0)u + \frac{1}{2} L_1(\mu)u + \cdots,$$

$$Q(\xi,\xi)=\begin{pmatrix} 2a_{20}\xi_1^2+2a_{11}\xi_1\xi_2 \\ 2b_{20}\xi_1^2+2b_{11}\xi_1\xi_2+2b_{02}\xi_2^2 \end{pmatrix}, \quad C(\xi,\xi,\xi)=\begin{pmatrix} 6a_{30}\xi_1^3+6a_{21}\xi_1^2\xi_2 \\ 6b_{30}\xi_1^2+6b_{21}\xi_1^2\xi_2 \end{pmatrix}.$$

It is worth noting that $Q(\cdot,\cdot)$ and $C(\cdot,\cdot,\cdot)$ are determined by the second-order Fréchet and third-order Fréchet derivations of operator $F(\cdot,0)$, respectively, see [25] for more details.

And the corresponding characteristic matrices are

$$\Delta_k(\lambda)=\begin{pmatrix} \lambda+\frac{k^2}{l^2}d_1-\overline{A} & -\overline{B} \\ -\overline{C} & \lambda+\frac{k^2}{l^2}d_2^{k_0^*}+\overline{A} \end{pmatrix}.$$

Obviously, $\lambda=0$ is a simple eigenvalue for $\Delta_{k_0^*}(\lambda)$, and $\lambda=\pm i\omega_0$ with $\omega_0=\sqrt{\mathrm{Det}_0}$ are eigenvalues for $\Delta_0(\lambda)$, while other eigenvalues have negative real parts according to Theorem 5.3. Then by straightforward calculations, we obtain

$$\vartheta_1=\begin{pmatrix} 1 \\ \dfrac{\overline{C}}{\frac{k_0^{*2}}{l^2}d_2^{k_0^*}+\overline{A}} \end{pmatrix}, \quad \varsigma_1=\frac{\frac{k_0^{*2}}{l^2}d_2^{k_0^*}+\overline{A}}{\frac{k_0^{*2}}{l^2}(d_1+d_2^{k_0^*})}\begin{pmatrix} 1 \\ \dfrac{\frac{k_0^{*2}}{l^2}d_1-\overline{A}}{\overline{C}} \end{pmatrix}^T,$$

$$\vartheta_2=\begin{pmatrix} 1 \\ \frac{i\omega_0-\overline{A}}{\overline{B}} \end{pmatrix}, \quad \varsigma_2=\frac{\overline{B}}{\overline{BC}+(i\omega_0-\overline{A})^2}\begin{pmatrix} \overline{C} \\ i\omega_0-\overline{A} \end{pmatrix}^T.$$

Therefore $\Phi=(\vartheta_1,\vartheta_2,\overline{\vartheta}_2)$ and $\Psi=(\varsigma_1,\varsigma_2,\overline{\varsigma}_2)^T$ satisfying $\varsigma_1\vartheta_1=1$, $\varsigma_2\vartheta_2=1$, $\overline{\varsigma_2}\vartheta_2=0$.

By [25], the normal form restricted on center manifold up to order 3 for reaction-diffusion system (3.1) at Turing-Hopf singularity is

$$\begin{cases} \dot{z_1}=a_1(\mu)z_1+a_{110}z_1^2+a_{023}z_2\overline{z}_2+a_{111}z_1^3+a_{123}z_1z_2\overline{z}_2+h.o.t., \\ \dot{z_2}=i\omega_0z_2+b_2(\mu)z_2+b_{120}z_1z_2+b_{112}z_1^2z_2+b_{223}z_2^2\overline{z}_2+h.o.t., \\ \dot{\overline{z}}_2=-i\omega_0\overline{z}_2+\overline{b_2(\mu)}\overline{z}_2+\overline{b_{120}}z_1\overline{z}_2+\overline{b_{112}}z_1^2\overline{z}_2+\overline{b_{223}}z_2\overline{z}_2^2+h.o.t.. \end{cases} \tag{5.3}$$

We omit the expressions $a_1(\mu)$, $b_2(\mu)$, a_{110}, a_{023}, a_{111}, a_{123}, b_{120}, b_{112}, b_{223} that can be computed directly by formulas in [25]. Instead, we derive concrete expressions for normal form (5.3) by fixing parameters. Then we present bifurcation diagrams of Turing-Hopf bifurcation and the corresponding phase portraits to exhibit spatiotemporal dynamics for diffusive system (3.1) near Turing-Hopf singularity.

We choose $\alpha=\frac{3}{4}$, $\gamma=\frac{1}{4}$, $u^*=\frac{1}{16}$, $l=6$, $d_1=0.005$. By direct calculations for system (3.1), we have $\delta_0=\frac{1}{104}$, $\beta=\beta^*=\frac{2535}{32}$, $k_0^*=6$, $d_2^{k_0^*}=\frac{187}{52}$, $v^*=\frac{1}{104}$, $\omega_0=\frac{\sqrt{179}}{104}$. Then, we have $k_1=6$ and $k_2=0$, and Turing bifurcation curve at $d_2-\delta$ plane is $d_2=\delta+\frac{373}{104}$, Hopf bifurcation curve is $\delta=\delta_0=\frac{1}{104}$, and Turing-Hopf bifurcation point is $(d_2,\delta)=(\frac{187}{52},\frac{1}{104})$.

Furthermore, for these given parameters, normal form (5.3) for (6, 0)-mode Turing-Hopf bifurcation truncated to order 3 is

$$\begin{cases} \dot{z_1} = \dfrac{4(\mu_1-\mu_2)}{3121} z_1 - 1.88 z_1^3 - 4.62 z_1 z_2 \overline{z}_2, \\ \dot{z_2} = i\dfrac{\sqrt{179}}{104} z_2 + \dfrac{(-89i+\sqrt{179})}{-179i+\sqrt{179}} \mu_2 z_2 - (1.75+1.97i) z_1^2 z_2 - (1.23+5.62i) z_2^2 \overline{z}_2, \\ \dot{\overline{z}_2} = -i\dfrac{\sqrt{179}}{104} \overline{z}_2 + \dfrac{(89i+\sqrt{179})}{179i+\sqrt{179}} \mu_2 \overline{z}_2 - (1.75-1.97i) z_1^2 \overline{z}_2 - (1.23-5.62i) z_2 \overline{z}_2^2. \end{cases} \tag{5.4}$$

Let $z_1 = \rho$, $z_2 = r\cos(\theta) + ir\sin(\theta)$ and $\overline{z}_2 = r\cos(\theta) - ir\sin(\theta)$ and drop the equation for θ, then (5.4) becomes

$$\begin{cases} \dot{r} = r(\dfrac{\mu_2}{2} - 1.75\rho^2 - 1.23r^2), \\ \dot{\rho} = \rho(\dfrac{4(\mu_1-\mu_2)}{3121} - 1.88\rho^2 - 4.62r^2). \end{cases} \tag{5.5}$$

Since $r \geq 0$, system (5.5) exhibits equilibria

$$\begin{aligned} &E_0 = (0,\, 0), \\ &E_1 = (0.64\sqrt{\mu_2},\, 0), \quad \text{for} \quad \mu_2 > 0, \\ &E_2^{\pm} = (0,\, \pm 0.026\sqrt{\mu_1-\mu_2}), \quad \text{for} \quad \mu_1 - \mu_2 > 0, \\ &E_3^{\pm} = (\sqrt{1.26\times 10^{-4}\mu_1 - 5.3\times 10^{-2}\mu_2},\, \pm\sqrt{-4.18\times 10^{-5}\mu_1 + 6.15\times 10^{-2}\mu_2}), \\ &\qquad \text{for} \quad 1.26\times 10^{-4}\mu_1 - 5.3\times 10^{-2}\mu_2 > 0, \ \ -4.18\times 10^{-5}\mu_1 + 6.15\times 10^{-2}\mu_2 > 0. \end{aligned}$$

Then, define critical bifurcation curves as follows

$$H_0:\ \mu_2 = 0; \quad T:\ \mu_2 = \mu_1; \quad T_1:\ \mu_2 = 0.00068\mu_1,\ \mu_2 \geq 0; \quad T_2:\ \mu_2 = 0.0024\mu_1,\ \mu_2 \geq 0.$$

The unfolding for (5.5) is similar to Case Ib in section 7.5 of [17]. Therefore, the bifurcation curves in $d_2 - \delta$ plane, still denoted by H_0, T, T_1, T_2, respectively, are shown in Fig. 5.1(a), where

$$\begin{aligned} &H_0:\ \delta = \delta_0, \quad T:\ \delta = \delta_0 + (d_2 - d_2^{k_0^*}), \\ &T_1:\ \delta = \delta_0 + 0.00068(d_2 - d_2^{k_0^*}),\ d_2 \geq d_2^{k_0^*}, \\ &T_2:\ \delta = \delta_0 + 0.0024(d_2 - d_2^{k_0^*}),\ d_2 \geq d_2^{k_0^*}. \end{aligned}$$

Therefore, the $d_2 - \delta$ plane is divided into six regions by these bifurcation curves. In each region, the dynamics of system (5.5) can be described by corresponding phase portraits in Fig. 5.1(b).

The equilibria E_0, E_1, $E_2^{\pm}$, $E_3^{\pm}$ of normal form system (5.5) correspond to the positive constant steady state, the spatially homogeneous periodic solution, the positive non-constant steady

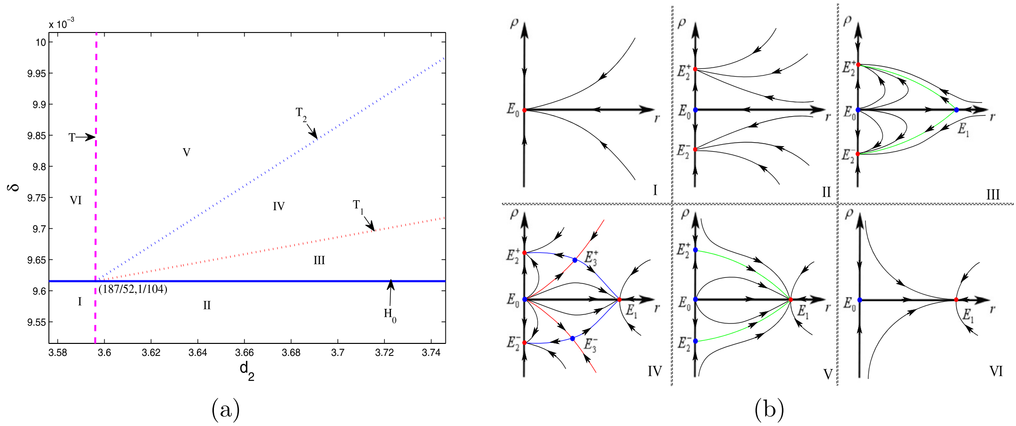

Fig. 5.1. Turing-Hopf bifurcation diagram in $d_2 - \delta$ plane for system (3.1) and corresponding phase portraits for system (5.5).

states and spatially inhomogeneous periodic solutions of system (3.1) (or system (5.1)), respectively. Thus, the dynamics of system (3.1) (or system (5.1)) near the Turing-Hopf singularity in $d_2 - \delta$ plane can be identified in terms of the dynamics of system (5.5).

We list all details of these cases as follows:

- **(a)** When $(d_2, \delta) \in$ I, system (5.1) exhibits monostability: a positive constant steady state, which is asymptotically stable in region I and unstable in other ones.
- **(b)** When $(d_2, \delta) \in$ II, system (5.1) exhibits bistability: two stable non-constant steady states. For different initial values, system (5.1) converges to one of these two stable non-constant steady states.
- **(c)** When $(d_2, \delta) \in$ III, an unstable spatially homogeneous periodic solution occurs, and system (5.1) still exhibits bistability: two stable non-constant steady states. Moreover, there exists a pair of heteroclinic orbits connecting spatially homogeneous periodic solution to non-constant steady states.
- **(d)** When $(d_2, \delta) \in$ IV, a pair of unstable spatially inhomogeneous periodic solutions occur, and system (5.1) exhibits tristability: two stable non-constant steady states and a stable spatially homogeneous periodic solution. Moreover, there exists two pair of heteroclinic orbits connecting spatially inhomogeneous periodic solutions to non-constant steady states or to the spatially homogeneous periodic solution. For different initial values, system (5.1) evolves from the unstable constant steady state to transient spatially inhomogeneous periodic solution, and finally to the stable spatially homogeneous periodic solution, or finally tends to one of non-constant steady states.
- **(e)** When $(d_2, \delta) \in$ V, a pair of unstable spatially inhomogeneous periodic solutions disappear and system (5.1) exhibits monostability: a stable spatially homogeneous periodic solution. Moreover, there exists a pair of heteroclinic orbits connecting non-constant steady states to the spatially homogeneous periodic solution.
- **(f)** When $(d_2, \delta) \in$ VI, a pair of unstable non-constant steady states disappear and system (5.1) exhibits monostability: a stable spatially homogeneous periodic solution. Moreover, there exists a heteroclinic orbit connecting the constant steady state to the spatially homogeneous periodic solution.

5.3. Codimension-3 bifurcations of reaction-diffusion system (3.1)

From Theorems 4.1, 4.3, 5.1, 5.2 and 5.3, we have the following theorem about Turing-Turing-Hopf bifurcation around $E^*(u^*, v^*)$.

Theorem 5.4. *If $\alpha < 1$, $\frac{1-\alpha-\gamma}{2} < u^* < \frac{1-\alpha}{2}$ and $(\alpha, \beta, \gamma, \delta) \in U_1$, then system (3.1) exhibits $(k-1, k, 0)$-mode Turing-Turing-Hopf bifurcation at $E^*(u^*, v^*)$ when $(d_1, d_2, \delta) = (d_1^{k-1,k}, d_2^{k-1,k}, \delta_0)$, $1 < k \le \overline{k}$, where all other eigenvalues of $P_k(\lambda) = 0$ have negative real parts besides two simple zero eigenvalues and a pair of pure imaginary eigenvalues.*

6. Discussion

In this paper, we investigated the diffusive Bazykin model (1.5) with Holling II functional response and predator self-limitation. After performing a complete stability and bifurcation analysis, our results revealed that system (1.5) exhibits complex dynamics and bifurcations, such as the global stability of a prey-only constant steady state or a unique positive constant steady state, the existence of Turing bifurcation, Hopf bifurcation, Turing-Turing bifurcation, Turing-Hopf bifurcation and Turing-Turing-Hopf bifurcation. More concretely, we first obtained an critical curve in (d_1, d_2)-plane that separates Turing stable and unstable regions. The curve is continuous and piecewise smooth, and the nonsmooth points corresponds to the critical values for Turing-Turing bifurcation. Hence, we established the sufficient and necessary condition for the occurrence of Turing instability. We found that the predators must diffuse faster than the prey for the occurrence of diffusive instability in system (3.1). Moreover, we can see that the larger the space domain, i.e. l, the more likely the system undergoes Turing instability. Next, we discussed the existence of k-mode Hopf bifurcation, studied the direction and stability of 0-mode Hopf bifurcation, which showed that model (1.5) exhibits temporal periodic patterns. Then, we derived the explicit formula of truncated normal form up to third order for Turing-Hopf bifurcation. A detailed analysis revealed that model (1.5) undergoes complex spatial, temporal and spatiotemporal patterns, including transient spatially inhomogeneous periodic solutions, monostability, bistability, tristability (a pair of positive non-constant steady states and a spatially homogeneous periodic solution), heteroclinic orbits (connecting a spatially inhomogeneous periodic solution to a non-constant steady state or a spatially homogeneous periodic solution, connecting a spatially homogeneous periodic solution to non-constant steady states and vice versa), etc. Meanwhile, numerical simulations, including transient, bistable and tristable patterns, verified and illustrated our theoretical results.

Our results about the global stability of a prey-only constant steady state or a unique positive constant steady state improved the corresponding results in Du and Lou [11] (see Theorems 3.2 and 3.5, Remarks 3.3 and 3.6). Cao and Jiang [8] considered complex spatiotemporal dynamics of a diffusive predator-prey model involving intraspecific competition and additional food supply to the predator. They studied Turing instability, Turing-Turing bifurcation and Turing-Hopf bifurcation. For Turing-Hopf bifurcation, they showed that the normal form is similar to Case II in section 7.5 of [17]. In our paper, we showed that the normal form for Turing-Hopf bifurcation is similar to Case Ib, moreover, we revised and obtained a more concise definition of the critical wavelengths in (4.4) for Turing instability, and proved the existence of Turing-Turing-Hopf bifurcation and the nonexistence of triple-Turing bifurcation (see Theorems 5.2 and 5.4).

Spatial patterns bifurcating from Turing bifurcation have been understood as early warning signals for tipping points or critical transitions toward an alternative state in various ecosystems

[40]. It is worth mentioning that the authors in [40,41,43] considered the change or transition of system state according to a single environmental condition (one parameter). In this paper, we discussed the joint effects of multiple bifurcation parameters on system state. From the two-parameter diagram for Turing-Hopf bifurcation in Fig. 5.1 and the corresponding transitions of spatiotemporal patterns, we can see that system (1.5) undergoes complex critical transitions and regime shifts when two parameters d_2 and δ vary around a tipping point, which is Turing-Hopf bifurcation point located on the Turing bifurcation curve. For example, a stable constant steady state to a stable spatially homogeneous periodic solution, or a stable constant steady state to one of two stable non-constant steady states depending on the initial values, or a stable constant steady state to one of two stable non-constant steady states or to a stable spatially homogeneous periodic solution depending on the initial values. System (1.5) can undergo from monostability to bistability, even tristability. Moreover, system (1.5) can exhibit complex transient dynamics, e.g., transient spatially inhomogeneous periodic solutions, etc. The linkage from bifurcation theory to transient dynamics caused by environmental changes needs much attention in future studies.

Acknowledgment

We would like to thank Fengqi Yi and Weihua Jiang for their helpful discussions, and Yongli Song for sending us a code to plot spatial patterns. JH's research was partially supported by NSFC (No. 11871235), and HW's research was partially supported by NSERC (RGPIN-2020-03911 and RGPAS-2020-00090).

References

[1] E. Avila-Vales, G. Garcia-Almeida, E. Rivero-Esquivel, Bifurcation and spatiotemporal patterns in a Bazykin predator-prey model with self and cross diffusion and Beddington-DeAngelis response, Discrete Contin. Dyn. Syst., Ser. B 22 (2017) 717–740.
[2] M. Banerjee, S. Ghorai, N. Mukherjee, Approximated spiral and target patterns in Bazykin's prey-predator model: multiscale perturbation analysis, Int. J. Bifurc. Chaos 27 (2017) 1750038.
[3] A.D. Bazykin, Structural and dynamic stability of model predator-prey systems, in: Int. Inst. Appl. Syst. Anal., Laxenburg, Austria, 1976.
[4] A.D. Bazykin, Nonlinear Dynamics of Interacting Populations, World Scientific, Singapore, 1998.
[5] H.W. Broer, V. Naudot, R. Roussarie, K. Saleh, Dynamics of a predator-prey model with non-monotonic response function, Discrete Contin. Dyn. Syst., Ser. A 18 (2007) 221–251.
[6] P.N. Brown, Decay to uniform states in ecological interactions, SIAM J. Appl. Math. 38 (1980) 22–37.
[7] X. Cao, W. Jiang, Turing-Hopf bifurcation and spatiotemporal patterns in a diffusive predator-prey system with Crowley-Martin functional response, Nonlinear Anal., Real World Appl. 43 (2018) 428–450.
[8] X. Cao, W. Jiang, Interactions of Turing and Hopf bifurcations in an additional food provided diffusive predator-prey model, J. Appl. Anal. Comput. 9 (2019) 1277–1304.
[9] S. Chen, J. Shi, J. Wei, Bifurcation analysis of the Gierer-Meinhardt system with a saturation in the activator production, Appl. Anal. 93 (2013) 1115–1134.
[10] Y. Du, S. Hsu, A diffusive predator-prey model in heterogeneous environment, J. Differ. Equ. 203 (2004) 331–364.
[11] Y. Du, Y. Lou, Qualitative behavior of positive solutions of a predator-prey model: effects of saturation, Proc. R. Soc. Edinb., Sect. A 131 (2001) 321–349.
[12] Y. Du, J. Shi, Allee effect and bistability in a spatially heterogeneous predator-prey model, Trans. Am. Math. Soc. 359 (2007) 4557–4593.
[13] T. Faria, Normal forms and Hopf bifurcation for partial differential equations with delays, Trans. Am. Math. Soc. 352 (2000) 2217–2238.
[14] T. Faria, W. Huang, J. Wu, Smoothness of center manifolds for maps and formal adjoints for semilinear FDEs in general Banach spaces, SIAM J. Appl. Math. 34 (2002) 173–203.
[15] H.I. Freedman, Stability analysis of a predator-prey system with mutual interference and density-dependent death rates, Bull. Math. Biol. 41 (1979) 67–78.

[16] H.I. Freedman, Deterministic Mathematical Models in Population Ecology, Marcel Dekker, New York, 1980.
[17] J. Guckenheimer, P. Holmes, Nonlinear Oscillations, Dynamical Systems, and Bifurcations of Vector Fields, Springer, New York, 1983.
[18] S. Guo, J. Man, Center manifolds theorem for parameterized delay differential equations with applications to zero singularities, Nonlinear Anal., Real World Appl. 74 (2011) 4418–4432.
[19] J. Hainzl, Multiparameter bifurcation of a predator-prey system, SIAM J. Math. Anal. 23 (1992) 150–180.
[20] J.K. Hale, Theory of Functional Differential Equations, Springer-Verlag, 1977.
[21] M. Haque, Ratio-dependent predator-prey models of interacting populations, Bull. Math. Biol. 71 (2009) 430–452.
[22] M. Haque, A detailed study of the Beddington-DeAngelis predator-prey model, Math. Biosci. 234 (2011) 1–16.
[23] M. Haque, Existence of complex patterns in the Beddington-DeAngelis predator-prey model, Math. Biosci. 239 (2012) 179–190.
[24] B.D. Hassard, N.D. Kazarinoff, Y.-H. Wan, Theory and Application of Hopf Bifurcation, Cambridge Univ. Press, Cambridge, 1981.
[25] W. Jiang, Q. An, J. Shi, Formulation of the normal form of Turing-Hopf bifurcation in partial functional differential equations, J. Differ. Equ. 268 (2020) 6067–6102.
[26] W. Jiang, X. Cao, C. Wang, Turing instability and pattern formations for reaction-diffusion systems on 2D bounded domain, Discrete Contin. Dyn. Syst., Ser. B 27 (2022) 1163–1178.
[27] X. Jiang, Z. She, S. Ruan, Global dynamics of a predator-prey system with density-dependent mortality and ratio-dependent functional response, Discrete Contin. Dyn. Syst., Ser. B 26 (2021) 1967–1990.
[28] J. Jin, J. Shi, J. Wei, F. Yi, Bifurcations of patterned solutions in the diffusive Lengyel-Epstein system of CIMA chemical reactions, Rocky Mt. J. Math. 43 (2013) 1637–1674.
[29] Y. Kuznetsov, Elements of Applied Bifurcation Theory, 3rd ed., Springer, New York, 2004.
[30] A. Leung, Limiting behaviour for a prey-predator model with diffusion and crowding effects, J. Math. Biol. 6 (1978) 87–93.
[31] A.J. Lotka, Elements of Physical Biology, Williams and Wilkins, Baltimore, 1925.
[32] M. Lu, J. Huang, Global analysis in Bazykin's model with Holling II functional response and predator competition, J. Differ. Equ. 280 (2021) 99–138.
[33] N. Min, W. Ni, H. Zhang, C. Jin, Long-time behavior of a diffusive prey-predator system with Beddington-DeAngelis functional response in heterogeneous environment, Z. Angew. Math. Phys. 70 (2019) 159.
[34] P. de Motoni, F. Rothe, Convergence to homogeneous equilibrium state for generalized Volterra-Lotka systems, SIAM J. Appl. Math. 37 (1979) 648–663.
[35] Y. Nishiura, Global structure of bifurcating solutions of some reaction diffusion systems, SIAM J. Math. Anal. 13 (1982) 555–593.
[36] S. Pal, M. Banerjee, V. Volpert, Spatio-temporal Bazykin's model with space-time nonlocality, Math. Biosci. Eng. 17 (2020) 4801–4824.
[37] R. Peng, F. Yi, X. Zhao, Spatiotemporal patterns in a reaction-diffusion model with the Degn-Harrison reaction scheme, J. Differ. Equ. 254 (2013) 2465–2498.
[38] R. Peng, M.X. Wang, Uniqueness and stability of steady states for a predator-prey model in heterogeneous environment, Proc. Am. Math. Soc. 136 (2008) 859–865.
[39] M. Rietkerk, J. van de Koppel, Alternate stable states and threshold effects in semi-arid grazing systems, Oikos 79 (1997) 69–76.
[40] M. Rietkerk, et al., Evasion of tipping in complex systems through spatial pattern formation, Science 374 (2021) eabj0359.
[41] M. Scheffer, Critical Transitions in Nature and Society, Princeton University Press, 2009.
[42] M. Scheffer, S.H. Hosper, M.-L. Meijer, B. Moss, E. Jeppesen, Alternative equilibria in shallow lakes, Trends Ecol. Evol. 8 (1993) 275–279.
[43] M. Scheffer, et al., Early-warning signals for critical transitions, Nature 461 (2009) 53–59.
[44] H. Shi, S. Ruan, Spatial, temporal and spatiotemporal patterns of diffusive predator-prey models with mutual interference, IMA J. Appl. Math. 80 (2015) 1534–1568.
[45] Y. Song, T. Zhang, Y. Peng, Turing-Hopf bifurcation in the reaction-diffusion equations and its applications, Commun. Nonlinear Sci. Numer. Simul. 33 (2016) 229–258.
[46] Y. Su, X. Zou, Transient oscillatory patterns in the diffusive non-local blowfly equation with delay under the zero-flux boundary condition, Nonlinearity 27 (2014) 87–104.
[47] A.M. Turing, The chemical basis of morphogenesis, Philos. Trans. R. Soc. Lond. B 237 (1952) 37–72.
[48] V. Volterra, Fluctuations in the abundance of species considered mathematically, Nature CXVIII (1926) 558–560.
[49] C. Wang, R. Liu, J. Shi, C.M. Del Rio, Spatiotemporal mutualistic model of mistletoes and birds, J. Math. Biol. 68 (2014) 1479–1520.

[50] J. Wang, J. Wei, J. Shi, Global bifurcation analysis and pattern formation in homogeneous diffusive predator-prey systems, J. Differ. Equ. 260 (2016) 3495–3523.
[51] M.X. Wang, Stationary patterns for a prey-predator model with prey-dependent and ratio-dependent functional responses and diffusion, Physica D 196 (2004) 172–192.
[52] J. Wu, Theory and Applications of Partial Functional Differential Equations, Springer, 1996.
[53] L. Yang, M. Dolnik, A.M. Zhabotinsky, I.R. Epstein, Spatial resonance and superposition patterns in a reaction-diffusion model with interacting Turing modes, Phys. Rev. Lett. 88 (2002) 208303.
[54] R. Yang, Y. Song, Spatial resonance and Turing-Hopf bifurcations in the Gierer-Meinhardt model, Nonlinear Anal., Real World Appl. 31 (2016) 356–387.
[55] F. Yi, J. Liu, J. Wei, Spatiotemporal pattern formation and multiple bifurcations in a diffusive bimolecular model, Nonlinear Anal., Real World Appl. 11 (2010) 3770–3781.
[56] F. Yi, J. Wei, J. Shi, Bifurcation and spatiotemporal patterns in a homogeneous diffusive predator-prey system, J. Differ. Equ. 246 (2009) 1944–1977.
[57] X.Z. Zeng, J.C. Zhang, Y.G. Gu, Uniqueness and stability of positive steady state solutions for a ratio-dependent predator-prey system with a crowding term in the prey equation, Nonlinear Anal., Real World Appl. 24 (2015) 163–174.
[58] Y. Zhang, J. Huang, Bifurcation analysis of a predator-prey model with Beddington-DeAngelis functional response and predator competition, under review.
[59] J. Zhou, Positive solutions of a diffusive Leslie-Gower predator-prey model with Bazykin functional response, Z. Angew. Math. Phys. 65 (2014) 1–18.